doi:10.1038/nature13687

Contents of Supplementary Text:

METHODS

Taxon sampling

We sampled 27 taxonomically diverse Neotropical bird lineages whose widespread distributions encompass lowland rainforests both east and west of the Andes (Fig. 1; Supplementary Figs. 1 - 27). The lineages we examined encompass both single, independently evolving species (and subspecies within them) and species complexes that include several closely related species (and subspecies within them). Because the alpha taxonomy of the lineages we examined is based on morphology, which can be an unreliable indicator of the amount of genetic differentiation, we use the term lineage to denote that both species and species complexes were examined in our analyses. We sampled the following lineages: *Piaya cayana* (Cuculidae), *Trogon rufus* (Trogonidae), *Ramphastos* species complex (Ramphastidae; data from 31,32), *Pteroglossus* species complex (Ramphastidae; data from 33), *Pyrrhura* (Psittacidae; data from 34), *Brotogeris* species complex (Psittacidae; data from 35), *Pyrilia* species complex (Psittacidae; data from 36), *Cymbilaimus lineatus* (Thamnophilidae), *Myrmotherula axillaris* (Thamnophilidae), *Sclerurus mexicanus* (Furnariidae), *Dendrocincla fuliginosa* (Furnariidae), *Glyphorynchus spirurus* (Furnariidae), *Xenops minutus* (Furnariidae), *Automolus ochrolaemus* (Furnariidae), *Colonia colonus* (Tyrannidae), *Attila spadiceus* (Tyrannidae), *Querula purpurata* (Cotingidae), *Lepidothrix coronata* (Pipridae), *Tityra semifasciata* (Tityridae), *Schiffornis turdina* (Tityridae), *Microcerculus marginatus* (Troglodytidae), *Henicorhina leucosticta* (Troglodytidae), *Tangara cyanicollis* (Thraupidae), *Tangara gyrola* (Thraupidae), *Tersina viridis* (Thraupidae), *Cyanerpes caeruleus* (Thraupidae), and *Chlorophanes spiza* (Thraupidae). We included closely related outgroup taxa for each lineage to identify the sister lineage(s). We included all available samples for each focal lineage that were deposited in the author's institutions. To supplement our geographic coverage of each lineage, we also obtained samples via genetic resource loans from other natural history museums (see acknowledgements) that have tissue collections. The large sample sizes in this study are the product of 30+ years of collecting expeditions in the Neotropics. Detailed locality information with geographic coordinates and museum tissue numbers are presented in Supplementary Table 17. This study was approved by the LSU Institutional Animal Care and Use Committee (IACUC protocol 09-001) and is in compliance with IACUC guidelines.

Sampling bias.- To evaluate comparative phylogeographic patterns across the Neotropical lowlands we directed our sampling to widespread lowland lineages whose distributions encompass both sides of the Andes. Although an assemblage of largely co-distributed lineages was expected to show concordant histories under the traditional model of landscape change driving speciation, we found that idiosyncratic histories are the predominant pattern. It seems likely that lineages having smaller distributions, which are presumably subject to the same stochastic processes as lineages having larger distributions, would also exhibit similar discordance in their phylogeographic patterns. There are many explanations for why some

lineages could have small distributions, including local population extinctions, limited habitat or resource availability, and competition. The generality of our results needs to be tested in other organisms, but the strength of our sampling design is that we have extensive taxonomic coverage with dense population-level sampling.

Speciation in birds.– We assume in this study that the first stage of speciation occurs via the geographic isolation of populations (i.e. allopatry). This is based on the overwhelming evidence for the predominance of this geographic mode of speciation for birds[3,37-39], and the fact that, to the best of our knowledge, there are no cases of parapatric or sympatric speciation documented in Neotropical birds[40]. In this study we examine how landscape features have interacted with species ecologies to create geographic isolation.

Mitochondrial DNA data collection

We extracted total DNA from ~ 25 mg of pectoral muscle tissue using the DNeasy Tissue Kit (Qiagen, Valencia, CA). We performed polymerase chain reaction (PCR) amplifications (25 μL) of the mitochondrial protein-coding cytochrome *b* (cyt *b*) gene, containing 2.5 μL template DNA (~50 ng), 1 μL each of the primers L14996 and H16064[41] (10 μM), 0.5 μL dNTPs (10 μM), 2.5 μL 10X with $MgCl_2$ reaction buffer, 0.1 Taq DNA polymerase (5 U/μL AmpliTaq; ABI, Foster City, CA), and 17.4 μL sterile ddH2O. The PCR temperature profile was an initial denaturation of 2 min at 94°C, followed by 35 cycles of 30 s at 94°C, 30 s at 45°–50°C, and 1 min at 72°C, with a final extension of 5 min at 72°C. We purified double-stranded PCR products using 20% polyethylene glycol and then cycle-sequenced using 1.75 μL 5X sequencing buffer (ABI), 1 μL sequencing primer (10 μM), 2.25 μL template, 0.35 μL Big Dye Terminator Cycle-Sequencing Kit (ver.3.1; ABI), and 1.65 μL sterile ddH2O. We cleaned reactions using Sephadex (G-50 fine) columns and we electrophoresed them on an ABI 3100 Genetic Analyzer. We manually assembled contigs for each individual using Sequencher (ver. 4.9; GeneCodes, Ann Arbor, MI), and we verified there were no stop codons in the coding region.

Data collection of ultraconserved elements

We analyzed orthologous and independently segregating nuclear loci published in a complementary study using massively parallel sequencing and sequence capture of ultraconserved elements (UCEs[42-45]). This data set comprised five of the lineages in our mtDNA data set: *Cymbilaimus lineatus, Microcerculus marginatus, Xenops minutus, Querula purpurata,* and *Schiffornis turdina*[46]. These five taxa were selected so as to have exemplars of both rainforest understorey and canopy foraging strata. Also, the variability in mtDNA gene tree height across the five taxa was representative of the variability observed across the 27-lineage data set. A complete description of the wet-lab protocol and bioinformatics used to assemble UCE data is available in Smith et al.[46]. Each lineage included 4-8 individuals and

had samples on both sides of the Andes, across the Isthmus of Panama, and across the Amazon River. The final UCE data sets included 166 orthologous loci that were shared across all five lineages. Divergence time analyses using coalescent modeling with migration found that cross-Andes divergence events occurred over the last few million years[46]: *Cymbilaimus lineatus*: 0.13 Ma (0.1-0.17); *Xenops minutus*: 2.50 Ma (2.22-2.82); *Schiffornis turdina*: 1.04 Ma (0.85-1.22); *Querula purpurata*: 0.19 Ma (0.16-0.22); *Microcerculus marginatus*: 1.51 Ma (1.11-1.90) (Supplementary Table 17). Divergence time estimates from UCE data tended to be more recent than mtDNA time estimates as predicted by coalescent theory, because divergence times from gene trees are expected to pre-date estimates from species trees[47]. Despite the expected disparity between estimates of divergence times from gene and species tree, the values from both data sets were highly correlated (R^2=0.69, $P < 0.0001$; Supplementary Table 17).

The Andes were the only dispersal barrier for which we had sufficient UCE sampling to further assess patterns of simultaneous divergence. We reduced each data set by removing haplotypes that represented phylogeographic structure that occurred prior or after cross-Andean divergence in order for the data to conform to the two population model in msBayes. We then removed loci from the reduced data set that contained >50% of missing data. The final data sets consisted of 129-163 loci: (*Cymbilaimus lineatus*: number of loci = 148; max length = 823 bp; min length = 34 bp; avg. length = 274 bp; *Microcerculus marginatus*: number of loci =156; max length = 804 bp; min length = 78 bp; avg. length = 437 bp; *Querula purpurata*: number of loci =156; max length = 978 bp; min length = 99 bp; avg. length = 584 bp; *Schiffornis turdina*: number of loci =129; max length = 931 bp; min length = 96 bp; avg. length = 509 bp; *Xenops minutus*: number of loci =163; max length = 961 bp; min length = 82 bp; avg. length = 428 bp).

Biogeographic areas

To examine how dispersal barriers in the lowlands of Central and South America influence diversification, we focused our sampling on avian taxa that are distributed on either side of landscape features previously recognized as barriers to lowland organisms. The majority of the sampled individuals were from humid lowland forests adjacent to these barriers. Due to variation in the distributions of our study taxa, however, some lineages contained population samples in foothills or open areas outside the humid lowlands. We assigned each individual sample to one of the biogeographic areas described below, and used this information in analyses to reconstruct ancestral ranges and to identify phylogeographic breaks in gene trees.

We used the general biogeographic areas proposed by Cracraft[48] and Haffer[49] and included additional areas that surround the core Amazonian biogeographic areas (Extended Data Fig. 1). The areas within Amazonia are largely delimited by the major tributaries of the Amazon River: Guiana – east of the Negro River through the entire Guiana Shield, Imerí – west of the Negro River to east of the Japurá River, Napo – the lowlands west of the Japurá River south through the area west of the Huallaga River and north of the upper Amazon

River, Inambari – the area east of the Huallaga River, south of the Amazon River, and west of the Madeira River, Rondônia – the area east of the Madeira River and west of the Tapajós River, Tapajós – the area east of the Tapajós River and west of the Xingu River, Xingu – the region east of the Xingu River and west of the Tocantins River, Belém – the area east of the upper Tocantins River, and the Atlantic Forest – the humid forest along the Brazilian Atlantic coast. Within the region west of the Andes: Magdalena – Magdalena valley in Colombia, including the Nechí and lower Cauca river basins, the Chocó – the area east of the Panamanian canal zone through the Darién and south to the humid forest along the Ecuadorian coast, Central America – the area west of the Panama canal zone to the Isthmus of Tehuantepec, and West of the Isthmus of Tehuantepec (West IoT) – the lowland forest of the Gulf Coast, and Pacific coast of Mexico.

To capture a more nuanced view of species distributions we assigned individuals to the following additional Neotropical areas: Andean Foothills – the foothill humid forests along the eastern side of the Eastern cordillera of Colombia and the Mérida cordillera and adjacent to the Llanos; Catatumbo – the southwest portion of the Maracaibo basin surrounded by Serranía de Perijá and Serranía de Motilones and the Mérida cordillera; Tumbes – the tropical deciduous dry forests along the Pacific coast of southwestern Ecuador and northwestern Peru; Orinoco Delta – the humid forests around the delta of the Orinoco River in Venezuela; Ilha Marajó in the mouth of the Amazon . The taxa *Tangara cyanicollis* (montane forests along the Andes and south central Amazonia), *Ramphastos ambiguus* (Eastern Andean foothills), *Pyrrhura rhodocephala* (Mérida cordillera), *Pyrrhura hoffmanni* (Chiriquí-Talamanca highlands), *Pyrrhura orcesi* (foothills of southwestern Ecuador), and *Pyrrhura albipectus* (Andean slopes of southeastern Ecuador) occur at higher elevations than the other species, so we included additional areas to reflect these differences: Western Andes – the foothill and cloud forests of Pichincha, Ecuador; Tachira – the foothill and cloud forests of Tachira, Venezuela; Southeast – the foothill and cloud forests of La Paz and Cochabamba, Bolivia; Northwest: the foothill and cloud forests of San Martín and Cajamarca, Peru; Eastern Andean foothills – foothill forests along the eastern flanks of the Andes from Bolivia to Ecuador.

Gene trees, divergence times, and ancestral area reconstruction

We generated gene trees and estimated divergence times using the program BEAST v.1.6.2[50] with an uncorrelated relaxed substitution rate based on an avian molecular clock[51] (lognormal distribution, mean = 0.0105, SD = 0.1), a coalescent: constant-size prior for the tree prior (except for *Ramphastos* and *Pteroglossus,* we used a speciation: Yule process tree prior), and a GTR + Γ finite-sites substitution model. We ran the analysis for 50 million generations and sampled every 2,500 generations. BEAST analyses were validated by performing multiple independent runs. We assessed MCMC convergence and determined the burn-in by examining ESS values and likelihood plots in Tracer v. 1.5[52]. We included sister species to ingroup taxa and in some cases we also included more distantly related outgroup taxa. Although our estimates are based on a single locus, comparisons of single versus

multilocus divergence time estimates in Neotropical birds indicate that temporal estimates based on mtDNA accurately reflect relative patterns of differentiation[53,54]. Because the mtDNA time estimates are gene divergences opposed to species divergences the inferred species ages are likely overestimates and represent the maximum ages of species. Thus, it is unlikely that multilocus species ages would be inconsistent with our conclusion of recent origins of species diversity. For the tree presented in Fig 2., we used a data set consisting of the inferred species (n=142) from our species delimitation analyses and followed the same approach that we used for the single lineage BEAST analyses, except that we used external calibrations for some nodes and fixed certain relationships identified from previous multilocus phylogenetic studies. We specified the prior distribution for the node representing the last common ancestor for: parrots and passerines (78.4 Ma[28]), *Glyphorynchus spirurus* and *Dendrocincla fuliginosa* (23 Ma[29]), and *Sclerurus mexicanus* and the other furnariids (33 Ma[29]). For each calibrated node prior we used a normal distribution with a standard deviation of 1.0 for the prior distribution.

We used a Bayesian phylogeographic model[55] in BEAST to infer spatial patterns of diversification and identify the most probable geographic origin of each of the 27 lineages. The Bayesian phylogeographic model implements ancestral reconstruction of discrete states on time-calibrated phylogenies. Within each of the 27 lineages we assigned individuals to a biogeographic area based on the geographic locality of the sample. A full description of biogeographic areas is discussed in the *Biogeographic areas* section above. We used the same parameter and prior settings as in the BEAST divergence-time analyses except that we restricted this analysis to only ingroup taxa and implemented the Bayesian Stochastic Search Variable Selection[55] (BSSVS). For the location.clock.rate prior we used a uniform prior (0 – 1). We used this Bayesian phylogeographic model to estimate whether a lineage had its ancestral origin west or east of the Andes. We determined the ancestral origin for a lineage by identifying the root node area with the highest posterior probability. Using the Bayesian phylogeographic model, we found that the most probable area of origin for 14 lineages was east of the Andes in the Amazon Basin, and for 13 it was west of the Andes in the Chocó and Central American region (Supplementary Table 17).

To confirm an effect of the landscape matrix on the genetic structuring of populations we compiled divergence times across five prominent biogeographic barriers (Fig. 1; Extended Data Figure 1): the Andes (west vs. east), the Isthmus of Panama (Chocó vs. Central America), the Negro River (Napo vs. Guiana), the upper Amazon River (Napo vs. Inambari), and the Madeira River (Inambari vs. Rondônia). We found that for each of the major biogeographic barriers (the Andes, Isthmus of Panama, or Amazonian rivers), 66 – 100% of the lineages exhibited phylogeographic breaks across them. Using the relative frequency of genetically undifferentiated populations across a barrier as a proxy of permeability, we found that the Andes (Supplementary Table 17; number of undifferentiated populations across barrier: n=0, disregarding single individuals that may represent incomplete lineage sorting or gene flow) were the least porous to dispersal, whereas Amazonian Rivers were the most permeable (n=17).

Bayesian species delimitation

The current taxonomy likely represents an inaccurate estimate of the standing avian diversity in the tropics[56,57], because the alpha taxonomy of many groups requires formal revision using modern methods (e.g. 54). We accounted for a potential effect of taxonomic bias in this study by delimiting putative species, irrespective of current taxonomy, using genetic data in a coalescent framework. Because evolutionary persistence is one of the variables we examined in this study, it is vital that within-lineage species be identified under a common framework[58].

We performed species delimitation analysis using the program bGMYC[59], a Bayesian implementation of the mixed Yule-coalescent model for species delimitation[60]. We explored different coalescent, Yule, and threshold values, and recovered similar results. For data sets with fewer than 50 individuals we lowered the default threshold value (number of species). We used the maximum clade credibility tree for each lineage and ran the program 100,000 generations using the single.phy function, discarding the first 15,000 generations as the burn-in. We performed MCMC diagnostics by checking likelihood plots of parameters and we ran each data set multiple times to assess the stability of the results. The program provides a posterior probability that two sequences belong to the same species, where a posterior probability of 1.0 between two sequences indicates there is a 100% probability that the two sequences belong to the same species and a posterior probability of 0.0 between two sequences indicates there is zero chance that the two sequences belong to the same species. We used a conservative approach for species delimitation and we classified species as clusters in the gene tree that had posterior probabilities $\geq$ 0.95 of belonging to the same species. The number of species inferred using Bayesian species delimitation ranged from 1-18 for each lineage (Supplementary Table 17; Supplementary Table 1).

To evaluate the impact of sample size on bGMYC species delimitation, we performed sensitivity analyses in which species diversity within each of the 27 lineages was estimated with bGMYC after excluding a fixed percentage of individuals in six different treatments. In the first treatment, we pruned 10% of the individuals (i.e. tree tips) randomly from each lineage's phylogeny using the R package APE[61]. For subsequent treatments, we successively increased the number of pruned individuals by an additional 10%, with the final treatment having 60% of its individuals removed. For each treatment we re-estimated species diversity using the previously described bGMYC approach (Supplementary Table 1; Extended Data Fig. 4). We then used t-tests to compare the distribution of species diversity estimated in the 27 lineages for all treatments. We found that the pruned data sets were not significantly different (two-tailed test) from the complete sampling distribution with up to 50% of the tips removed (Supplementary Table 2). The results were equivalent when we used a nonparametric K-S test instead of a t-test.

Although there have been some recent refinements, the bulk of the current taxonomy of the study lineages was established in the 1800s by examination of phenotypic variation in museum study skins. Because taxonomists tended to assign a name to any geographic variant, the current taxonomy (species and subspecies within lineages) is undoubtedly an overestimate

of the number of species within each lineage. In contrast, because of its dependence on dense genetic sampling and our conservative threshold for accepting genetic clusters as species, the Bayesian delimitation method likely underestimates diversity. The 'true' species diversity lies somewhere in between these extremes of diversity. Despite the potential for issues of under- or over-estimating species diversity, the number of inferred species using bGMYC was highly correlated (R^2 = 0.77) with the number of described taxa (species and subspecies). This result suggests that the bGMYC analyses identified taxa that are diagnosable with genetics as well as morphological and vocal characters. It is likely that future taxonomic revisions will elevate many of these inferred species or subspecies within the 27 lineages to biological species status[56,57]. For example, it has been proposed that the species *Schiffornis turdina* in our study be split into five separate biological species[62]. For subsequent analysis, we treated all taxa within the 27 lineages as species.

Testing for simultaneous divergence

To estimate the temporal patterns of disparity in isolation across the dispersal barriers, we used a hierarchical approximate Bayesian computation approach (hABC) that accounts for gene tree/population divergence disparity under the coalescent while allowing independence across species in demographic parameters. We used an implementation of hABC in the software msBayes[63] and we analyzed the sequence data for multiple co-distributed population pairs jointly under a hierarchical divergence model. We tested for simultaneous divergence and estimated the number and relative ages of co-divergence pulses between pairs of neighboring regions divided by biogeographic dispersal barriers.

We used summary statistics from msBayes to compare observed patterns in sequence diversity with data simulated under a model of ancestral populations splitting into two daughter populations (without subsequent migration) simultaneously for all species. Each simulation run involved (i) drawing a random value of Ψ (number of divergence events across all population pairs in a data set) from its discrete uniform hyperprior distribution; (ii) drawing divergence times $\tau, ..., \tau_n$ for each of the n population-pairs conditional on this instance of Ψ (i.e. all species will have the same τ if Ψ=1 whereas each population-pair draws from the $\tau, ..., \tau_\Psi$ possible times when Ψ>1 conditional on each of these Ψ times having at least one population splitting), (iii) drawing species-specific demographic parameters independently from shared prior distributions (independent of Ψ); (iv) simulating multispecies data given the randomly drawn hyperparameters as well as sample sizes, fragment lengths and known generation times for each species and (v) generating vectors of summary statistics from these simulated data sets.

Posterior distributions for the hyperparameters of interest – Ψ, shared τ ($\tau, ..., \tau_\Psi$), and $\sigma^2/\bar{\tau}$ - were generated by first applying a rejection step using the Euclidian distance between vectors of observed and simulated summary statistics, followed by a method of weighted local linear regression for continuous parameters and weight logistical polychotomous regression for discrete parameters[64]. Population divergence times (τ_i) for each of the 27

lineages were scaled relative to their effective population sizes (N_i), i.e. $t = \tau_i 2N_i g$, where g is the generation time in years. To report divergence times across co-diverging lineages in global coalescent time units (i.e. τ scaled by N generations) given that each lineage has different values of N_i, each τ_i was rescaled to the same global scale using the relationship $\tau_= \tau_i \theta_i /b$, where b is, the global scalar of q. For example, if a population pair had a small N_i and large τ_i (in units if 2 N_ig), its globally expressed divergence time τ would be directly comparable to a population pair with an equal divergence in absolute time but with differing N_i (and hence differing τ_i).

Using single-locus data from multiple population-pairs results in a 'borrowing strength' for improved parameter estimation[65-67], which is akin to increasing statistical power of single-species estimates of parameters by sampling greater numbers of unlinked genetic loci. The pattern and degree of dissynchrony in divergence times is captured by hyperparameters; Ψ, which quantifies the number of divergence times; $\sigma^2/\bar{\tau}$, the index of dispersion quantifying normalized variability in divergence times; and the vector of co-divergence times $\tau, ..., \tau_\Psi$ conditional on Ψ. We assumed uniform prior distributions for all species-level parameters with upper bounds that are not greater than the maximum gene-tree divergence estimated from BEAST, such that the ABC sampler efficiently drew plausible population divergence times < gene-tree divergence times[67,68] to avoid downwardly biased estimates in Ψ[69]. To further demonstrate that the priors were able to reproduce the main features of the observed data[66,70], we further obtained a graphical check using the first two principal components of the summary statistics calculated from 1,000 random draws from each prior. The hyperprior for the hyperparameter Ψ was discrete uniform and upwardly bound by *n*, the number of species-pairs in any particular analysis; $\Psi = (1,n)$. Scaled effective population sizes for both ancestral populations (θ_a) and descendent pairs of daughter populations (θ_1 and θ_2) were allowed to vary independently.

We performed hABC analyses on both single locus mtDNA data (Extended Data Fig. 2) and data from orthologous, independently segregating nuclear UCEs (Extended Data Fig. 3). We identified sister population-pairs from the BEAST mtDNA gene trees across five biogeographic barriers: the Andes (n=29), the Isthmus of Panama (n=14), the Negro River (n=17), the upper Amazon River (n=14), and the Madeira River (n=14). We did not include sister populations-pairs that only had one sample on each side of the Andes. In some taxon-pair comparisons we removed haplotypes representing phylogeographic structure occurring after divergence in order for the data to conform to the two-population model of msBayes. For the expanded data matrix of UCE data, we assembled a data set of five lineages and 129 – 163 UCEs: *Cymbilaimus lineatus* (n = 148), *Xenops minutus* (n = 163), *Schiffornis turdina* (n = 129), *Querula purpurata* (n = 155), and *Microcerculus marginatus* (n = 156). For the UCE matrix our sampling only permitted testing simultaneous divergence across the Andes.

For each data set of population pairs split by a particular barrier, we initially ran a separate msBayes analysis with a discrete uniform prior on Ψ, with the prior Ψ values ranging

from 1 (simultaneous divergence) to the maximum number of divergences (Ψ= number of pairs) all being equally likely. Comparisons of the posterior probabilities of a synchronous pulse of divergence ($\sigma^2/\bar{\tau} \leq 0.01$; M_1) and asynchronous divergence ($\sigma^2/\bar{\tau} > 0.01$; M_2) were made with Bayes Factors ($B(M_1, M_2)$), with values of $B(M_1, M_2) < 1/10$ and $1/10 < B(M_1, M_2) < 1/3$ being interpreted as strong and moderate support for asynchronous divergence, respectively[71]. For all calculations of Bayes factors, we used the ABC approximation $B(M_1, M_2) = Pr(M_1|D)/Pr(M_2|D)/Pr(M_1)/Pr(M_2)$, where the posteriors of the two models $Pr(M_1|D)$ and $Pr(M_2|D)$ are approximated from the set of 1,000 summary statistic vectors passing the final ABC filter. For the mtDNA data sets we performed additional msBayes analyses conditional on all Ψ values having > 0.02 posterior probability in order to visually represent the uncertainty underlying the estimates of co-divergence pulse times.

We used a rate of 2.1% sequence divergence per million years for analyses with mtDNA[51] and 0.2% per million years for analyses with UCEs[46], and mean substitution-rate uniformity across species with a gamma-distributed rate variation across loci within species as in Huang et al.[63]. We note that the results presented herein are not dependent on absolute molecular dates nor on the accuracy of this molecular clock calibration, but that DNA substitution rate variation across species could result in incorrectly rejecting a history of synchronous divergence.

For the mtDNA data, we used four summary statistic classes calculated across all population pairs that have previously been shown to capture information about co-divergence using simulations[65]: average pairwise diversity scaled per base-pair (π), average net diversity between populations scaled per base-pair (π_{net}), Wattersons's theta scaled per base-pair (θ_W; the number of segregating normalized for sample size) and δ, the denominator of equation 38 in Tajima[72] (Tajima's D), where *S*, the number of segregating sites is scaled per base-pair rather than per locus. For the UCE data, only one summary statistic class was used (π_b; average pairwise differences between populations) to accommodate loci that lacked polymorphism within populations. To allow this vector of summary statistics to be order-independent we used the ranking scheme of Huang et al[63]. Summary statistics of mtDNA are in Supplementary Tables 3-7 and π_b values from UCEs are available in Supplementary Table 17. Bayes factors for model comparisons are presented in the main text.

Ecological and historical variables

The total number of variables used in our phylogenetic generalized least-squares (PGLS) analyses was dictated by the sample sizes of the response variables. Our complete data set consisted of ~2500 samples from 27 independent lineages, but to avoid a potential correlation between divergence estimates extracted from the same phylogeny we binned divergence estimates into three independent classes of barriers: the Andes, Isthmus of Panama, and Amazonian Rivers. This reduced set of response variables limited the number of potential predictor variables that could be included in multivariate models.

The diversity of ecological and historical variables that can be collected for Neotropical birds is relatively large. Published data sets describing species-specific diet,

habitat, relative abundance, distribution, elevational range, and range size are available[73]. Morphological data that may reflect ecological differences, such as body size and wing shape, can be obtained from museum specimens. Additionally, variables that capture aspects of a lineage's evolutionary history, such as clade age, colonization time of an area, diversification rate, and ancestral area of origin, can be inferred from phylogenetic data. Because the number of potential predictor variables was larger than the sample sizes of the genetic metrics to be modeled, we selected two ecological and two historical variables that are known or predicted to influence genetic differentiation.

The ecological variables we examined initially were foraging stratum, foraging guild, habitat breadth, maximum elevation, niche breadth, and hand-wing index from museum specimens. Previous work found that foraging stratum and foraging guild were correlated and that foraging stratum was a more significant predictor of genetic differentiation[11]. Further, sample sizes of the differing foraging guilds were skewed, with only a few omnivores (frugivore: n=10, insectivore: n=12, and omnivore: n=5), so we did not retain this variable for further analysis. Previous work also found that classifying species by their presence in forest edge or várzea forest, maximum elevation, and the total numbers of preferred habitats were poor predictors of levels of genetic divergence across barriers[11]. However, the lack of an apparent influence of habitat on genetic differentiation may be due to the use of categorical variables that provide a course approximation of habitat preference. To further evaluate the relationship between environmental preferences and genetic divergence, we included niche breadth, a continuous variable estimated from climatic suitability values of ecological niche models, as a second ecological variable. Abundance, another potentially important variable that distinguishes between species with large and small populations, was not included because the lineages used in this study all exhibit relatively high abundance. Therefore, the two ecological variables retained for all analyses were foraging stratum and niche breadth.

The historical variables we examined were stem age, crown age, and area of ancestral geographic origin. Stem and crown age are proxies for how old a lineage is. Stem age is the age of the last common ancestor of an ingroup and its sister clade and crown age is the timing of the basal divergence within an ingroup[74]. Stem ages are expected to be more biased by extinction, but capture the length of time between a last common ancestor and the diversification of a crown clade, which provides insight into lineage persistence across deeper time than crown age. Alternatively, crown ages at the phylogeographic-scale are more likely to be subject to uncertainties associated with lineage sorting and reflect patterns retained within an ingroup. We observed a similar pattern between species diversity and age regardless of whether we used crown or stem age (Supplementary Table 12). Additionally, for some of the lineages in our data set the crown age and the cross-Andes divergence event were the same node in the gene tree. Thus, we opted for stem age instead of crown age as the estimate of lineage age. Assuming extinction rates are comparable among lineages and that diversification within lineages is density-independent, stem ages can be interpreted as a measure of evolutionary persistence.

We also included area of ancestral geographic origin because it allowed us to compare patterns between lineages that originated in an area and those that dispersed into an area. In summary, we selected two ecological (foraging stratum and niche breadth) and two historical (stem age and ancestral area of origin) variables for our phylogenetic generalized least-squares analyses because these variables are predicted to influence genetic differentiation and because they adequately reflect ecological and evolutionary differences among lineages (Supplementary Table 8). A complete description of each variable is listed below.

Foraging stratum – We binned lineages into two foraging stratum categories: understorey and canopy (*sensu* 11). Understorey birds are species that typically forage from the ground through the midstorey and canopy birds typically forage from the midstorey to the canopy (*sensu* 73). The foraging stratum of species has been shown to influence genetic differentiation across biogeographic barriers[11], because species that inhabit the canopy of rainforests are typically better dispersers than species that inhabit the understorey. Thus, the prediction is that poor-dispersing understorey birds will exhibit higher genetic differentiation or older divergence times across biogeographic barriers in the Neotropical lowlands than more dispersive canopy species[11]. We assigned 16 lineages to the canopy category and 11 to the understorey category.

Niche breadth – We generated ecological niche models (ENMs) for each of the 27 lineages using temperature and precipitation variables (Supplementary Figs. 1-27). To build an ENM for each lineage, we used latitude-longitude coordinates obtained from voucher specimens that had genetic samples. For lineages with smaller sample sizes, we supplemented locality records by including observational records from the xeno-canto (http://www.xeno-canto.org/) online database of bird songs. Lineage and sample: *Piaya cayana* (n=128), *Trogon rufus* (n=53), *Ramphastos* (n=107), *Pteroglossus* (n=89), *Pyrrhura* (n=75), *Brotogeris* (n=84), *Pyrilia* (n=75), *Cymbilaimus lineatus* (n=53), *Myrmotherula axillaris* (n=85), *Sclerurus mexicanus* (n=38), *Dendrocincla fuliginosa* (n=82), *Glyphorynchus spirurus* (n=95), *Xenops minutus* (n=91), *Automolus ochrolaemus* (n=62), *Colonia colonus* (n=41), *Attila spadiceus* (n=52), *Querula purpurata* (n=38), *Lepidothrix coronata* (n=45), *Tityra semifasciata* (n=65), *Schiffornis turdina* (n=77), *Microcerculus marginatus* (n=62), *Henicorhina leucosticta* (n=40), *Tangara cyanicollis* (n=40), *Tangara gyrola* (n=53), *Tersina viridis* (n=57), *Cyanerpes caeruleus* (n=53), and *Chlorophanes spiza* (n=50).

We used the bioclimatic variables from the World-Clim data set (v. 1.4) with a resolution of 30 arc-seconds[75]. Using the correlation analyses in ENMtools[76], we found that nine of the variables were highly correlated with other variables ($R > 0.9$); therefore, we used 10 of the 19 temperature and precipitation variables (BIO1, BIO2, BIO3, BIO5, BIO7, BIO12, BIO14, BIO15, BIO18, and BIO19). We generated ten replicate models for each taxon using the maximum entropy algorithm in Maxent 3.3.3[77]. For each model 75% of the points were used for model training and 25% were used as test points. The area under the

receiver operating characteristic (ROC) curve was close to one, with the average AUC ranging 0.714-0.915 across the 27 lineages (Supplementary Table 17).

We used the average ENM from the ten replicate models for each lineage to estimate niche breadth[78] in ENMtools[76]. Niche breadth was based on the Maxent predictions of climate suitability for each lineage. Species with wider niche breadths may face lower ecological resistance in dispersing across the landscape and may have lower genetic differentiation across their ranges (e.g. 79). We assessed whether range size, a variable often correlated with metrics of species diversity (e.g. 80), was correlated with niche breadth by calculating the area (km^2) occupied by each bird lineage using digital range maps[81] in ArcGIS10. In some instances there were overlapping ranges among species within lineages (e.g. *Brotogeris*), so we summed the area of overlapping ranges. We found that niche breadth was correlated with lineage range size ($R^2 = 0.62$), demonstrating that the relationship between genetic divergence and range size was likely captured using niche breadth. From our estimates of niche breadth, we identified a wide variability in values across lineages, ranging from 0.29-0.68 (Supplementary Table 17).

Lineage age - We used the BEAST maximum credibility trees to identify the divergence time of each ingroup from its sister group. This divergence time is referred to as the stem age, and represents the length of time in which a lineage has been evolving independently from its last common ancestor. Species diversity at a given area is predicted to increase with the time a clade has been in the area[21]. However, the relationship between stem age and the timing of cross-barrier divergence has not been evaluated. Thus, older and younger lineages may show differing patterns of diversification across the landscape because a lineage may have had more time for diversification.

Ancestral geographic origin - We classified lineages as having their ancestral geographic origin in the lowlands west or east of the Andes based on the results from the BEAST phylogeographic modeling (see *Gene trees, divergence times, and ancestral area reconstruction* section**)** that provided a probability for geographic location of the root state. The influence of ancestral origins on patterns of genetic differentiation has not been fully explored. However, diversification rates have been shown to increase after lineages have colonized regions, such as the Andes[82] or across Wallace's line[83]. Lineages that originated east of the Andes may show different patterns than lineages that originated west of the Andes.

River - In the PGLS analyses examining divergence levels across Amazonian rivers, we included a River variable to correct for potential differences among the rivers (the Amazon, Negro, and Madeira Rivers) included in the model. The amount of gene flow across each river likely varies and divergence-time patterns may vary among riverine barriers. Thus, by treating the barrier that each divergence time was estimated across as a variable, we were able to account for among-river variability in temporal patterns.

Phylogenetic comparative analysis of species diversity and cross-barrier divergence levels

We tested whether the observed variation in species diversity and cross- barrier divergence times could be attributed to species ecology and history. We employed a phylogenetic generalized least-squares (PGLS) analysis to evaluate the effect of two ecological and two historical variables on two metrics of genetic differentiation: 1) a species-diversity metric (presented in the main text), and 2) a genetic divergence metric of the level of differentiation across major dispersal barriers (not presented in main text): the Andes, the Isthmus of Panama, the upper Amazon River, the Negro River, and the Madeira River. The divergence metric allowed us to assess the effects of history and ecology on specific dispersal barriers.

For the divergence metric we assessed three independent models that examined the effect of historical and ecological variables on genetic divergence levels across 1) the Andes (m_1), 2) the Isthmus of Panama (m_2), and 3) three Amazonian rivers (m_3). Sample sizes are provided in Supplementary Table 8. For the species-diversity metric, we ran a model that examined the effect of historical and ecological variables on the overall number of species in each lineage (m_4) using bGMYC species. All variables are discussed in detail in the *Ecological and historical variables* section of the Methods. In all models, we treated predictor variables as fixed effects and we accounted for the statistical non-independence of lineage data by including a phylogenetic correction.

We performed PGLS analyses using the caper package[84] in the R programming language[85]. The phylogenetic signal in the data is controlled by the parameters lambda, kappa, and delta. We optimized the value for lambda using maximum likelihood and we kept the default values for kappa (1.0) and delta (1.0). We performed both univariate and multivariate tests allowing us to assess relationships between a single variable and to identify the relative significance of each variable. We built two divergence data sets for the Isthmus of Panama and Amazonian rivers models, one that included only divergence times between sorted populations on each side of the barrier, and a second data set that included unsorted populations across barriers that had divergence times estimated to be zero. The Andes data set did not contain divergence times estimated to be zero. For the multivariate models, we included two ecological variables (foraging stratum and niche breadth) and two historical variables (ancestral origin and lineage age) that are predicted to influence genetic differentiation. We also included a term *rivers* to account for variation across rivers in the response variable in the model m_3. We performed preliminary analyses that examined the fit of the data to a model with and without square root and log conversions to the data. In cases where the conversion reduced the residual variance of a model, we converted variables in the final models. For models m_1-m_3, we log transformed the cross-barrier divergence times and lineage age. For model m_4, we square root converted species diversity. For the stem age estimates in m_4 and the cross barrier divergence times in m_1-m_3 we ran additional models using the time estimated from the low and high 95% HPD to assess how robust patterns were to uncertainty in molecular dating. Raw data used in these analyses are available in

Supplementary Table 17. Differences between sample sizes between the PGLS analyses and hABC analyses are attributed inadequate sample sizes for population genetic summary statistics or our inability to identify node age in a gene tree. We built phylogenies in BEAST using the settings described in the divergence time section of the methods for models m_1-m_4. For each model, we built a phylogeny with the appropriate number of tips to match the number of observations of species diversity and cross-barrier divergence levels. For preliminary analyses, we used 100 trees from the posterior distribution as input in the PGLS analyses. We found that phylogenetic uncertainty in the posterior distribution of trees had minimal influence on our model parameter estimates (results not shown); therefore we report model results from runs using a single tree.

For multivariate models, we estimated Akaike information criterion (AICc) scores with a correction for sample size for models containing a complete list of variables and the AICc score for each model without each of the predictor variables. We assessed the relative importance of each variable by calculating Δ AICc = $AICc_a$ - $AICc_f$, where Δ AICc is the change in AICc between the model without a particular predictor variable ($AICc_a$) and the full model ($AICc_f$). Models with a Δ AICc > 2 are deemed to be significantly different than the full model. For some of our multivariate models, we had a low sample size, which may decrease their power to accurately detect significant effects[86]. To assess potential biases caused by low sample sizes in the multivariate models, we compared the results between the univariate and multivariate models (Table 1; Supplementary Tables 9-12). Overall, we obtained similar parameter estimates for most variables using both types of models (Table 1; Supplementary Tables 9-12), indicating that the relationship between the response and predictor variables was detectable with low sample sizes. In the species diversity model (m_4), however, Ancestral Origin was significant ($\alpha = 0.05$) in the univariate model (Supplementary Table 12), but not in the multivariate model (Table 1).

Influences of sample size and species-diversity on PGLS analyses

To evaluate whether the differential sample sizes between understorey and canopy lineages biased our results, we conducted additional analyses on species diversity estimates from the pruned data sets in which 10-60% of the individuals were removed randomly (Extended Data Fig. 4; Supplementary Table 1). To examine how the pruning treatments influenced the relative importance of each predictor variable, we performed PGLS analyses for the model examining species diversity on each treatment. We found that lineage age and foraging stratum remained significant predictor variables with up to 30% and 50%, respectively, of the individuals removed randomly (Supplementary Table 16). We also ran the model with the low and high value of the 95% HPD to examine whether the uncertainty surrounding stem age influenced the results. We recovered the same pattern, with a few exceptions, that stem age and foraging stratum were significant variables when we used the low and high values of the 95% HPD (Supplementary Table 16). Based on our collective results, the diversity-lineage age relationship is robust to species diversity estimates with up

to 30% of the samples being randomly removed and the uncertainty surrounding stem age. Foraging stratum remained significant with up to 50% of the individuals in each data set being randomly pruned.

Influence of undifferentiated populations across barriers

Divergence times were extracted from lineages that had differentiated across barriers; however, there were taxa that were not genetically diverged across these same barriers. We explored how these undifferentiated taxa influenced our model interpretations by running additional analyses that included these taxa by setting their divergence times to zero. There were undifferentiated populations across the Isthmus of Panama and Amazonian rivers, but not across the Andes. For these models, we changed estimates of divergence time of 0 to 0.1 in order to log-transform the values. In the Isthmus of Panama model (m_2), we obtained overall similar results between the models with and without zero divergence times (Supplementary Table 14). The only significant difference was that when the 95% HPD high for cross-Isthmus divergences was used ancestral origin changed from 11.4624 (Supplementary Table 14a, Δ AICc C) to 0.2148 (Supplementary Table 14b, Δ AICc C). In the Amazonian rivers model (m_3), ancestral origin also became not significant when zero divergence times were included (Supplementary Table 15), but stem age became significant for the mean (Supplementary Table 15b, Δ AICc A=2.9226) and 95% HPD high value (Supplementary Table 15b, Δ AICc C=3.8067). The lack of significance of Ancestral Origin in the Amazonian river model (m_3) with zero divergences is likely attributable to recent dispersal events across rivers in taxa that originated in Amazonia.

Effects of ecology and evolutionary history on diversification

Overall, we obtained similar parameter estimates for the majority of variables, using either the univariate or multivariate model (Table 1; Supplementary Tables 9-11 A & B; Supplementary Table 12) showing there were significant effects of individual histories and ecologies on the timing of diversification in most models. The only model that had no significant effects was the cross-Andes divergence model (m_1), which measured the effect of the least permeable dispersal barrier, the Andes Mountains (Supplementary Table 9). This result suggests that our estimate of dispersal ability and the scale of the historical variables we included had no detectable influence on the timing of cross-Andes divergence. Lineage age did show a positive, albeit non-significant, relationship with cross-Andes divergence, which would suggest that the dispersal across the Andes was a function of how long a lineage has been in the landscape. Given the results of our cross-Andes divergence model comparisons, however, the non-significance of any of the variables suggests that diversification across the Andes is most consistent with stochastic processes. We found that lineage age (Δ AICc A-C =6.4665-7.1862; Supplementary Table 14) had a significant positive effect in the model assessing genetic divergence across the Isthmus of Panama, and that geographic region of origin (Δ AICc A-C = 11.4624-11.9199; Supplementary Table 14; Supplementary Fig. 28) was also significant. Ecologically, foraging stratum significantly influenced the timing of

divergence across Amazonian rivers (foraging stratum, Δ AICc A-C =8.2501-10.0460; Supplementary Table 15), as did the region of ancestral origin (Δ AICc A-C = 8.0215-9.6711; Supplementary Table 15; Supplementary Fig. 28). Niche breadth was not a significant effect in any of the models assessing cross-barrier divergences (Supplementary Tables13-15). In sum these results suggest that divergence across barriers is determined by stochasticity, the amount of time a taxon is in the landscape, its geographic origin, and/or its dispersal ability.

As discussed in the main text, species diversity, as defined by coalescent analyses within the 27 lineages, was predicted by lineage age (Supplementary Table 16). This pattern was robust to the uncertainty surrounding stem age and the random pruning of tips from the data sets (Supplementary Table 16). Ecologically, we found that foraging stratum (Supplementary Table 16) had a significant effect on species diversity, with lineages restricted to the forest understorey containing significantly higher species diversity than canopy lineages (Table 1, Foraging Stratum – Understorey, coefficient= 0.5188, $P = 0.0178$) . The higher diversity in understorey birds than canopy birds appears not to be attributable to differences in range sizes because we tested for a significant difference in range size between understorey and canopy lineages and the test was not significant (two-sided Student's t-Test: $t = 1.6250$; $P = 0.1191$). Niche breadth was not identified as a significant effect in the species diversity model (Supplementary Table 16).

Supplementary Table 1 | List of lineages with number of described taxa (species and subspecies), number of inferred species with complete and pruned data sets, and total number of individuals in each data set.

Lineage	Foraging Stratum	Number of described taxa[87] (species & subspecies)	Number of species from bGMYC Complete sampling	10% pruned	20% pruned	30% pruned	40% pruned	50% pruned	60% pruned	Sample size n
Attila spadiceus	Canopy	12	2	2	2	2	2	2	3	108
Brotogeris	Canopy	17	6	7	6	6	6	5	5	54
Chlorophanes spiza	Canopy	7	2	2	3	2	2	2	2	72
Colonia colonus	Canopy	5	3	3	3	3	3	2	2	18
Cyanerpes caeruleus	Canopy	5	1	1	1	1	1	1	2	39
Cymbilaimus lineatus	Canopy	3	2	2	2	2	2	2	2	48
Piaya cayana	Canopy	14	4	4	3	4	3	4	3	49
Pteroglossus	Canopy	23	7	4	3	5	3	4	3	52
Pyrilia	Canopy	9	6	7	7	6	5	3	6	29
Pyrrhura	Canopy	48	18	15	4	4	2	2	3	81
Querula purpurata	Canopy	1	2	2	2	2	2	2	2	49
Ramphastos	Canopy	17	7	8	6	6	6	5	4	35
Tangara cyanicollis	Canopy	7	2	2	2	2	2	2	2	47
Tangara gyrola	Canopy	9	3	3	3	3	3	3	2	90
Tersina viridis	Canopy	3	2	2	2	2	2	2	2	27
Tityra semifasciata	Canopy	9	3	3	3	3	3	3	2	52
	Average	11.81	4.38	4.19	3.25	3.31	2.94	2.75	2.81	53.13
	Std. Dev.	11.34	4.13	3.56	1.69	1.66	1.48	1.18	1.22	23.99

(continued)

Lineage	Foraging Stratum	Number of described taxa (species & subspecies)	Number of species from bGMYC Complete sampling	10% pruned	20% pruned	30% pruned	40% pruned	50% pruned	60% pruned	Sample size n
Automolus ochrolaemus	Understorey	8	5	5	4	5	4	3	3	166
Dendrocincla fuliginosa	Understorey	14	7	7	6	5	5	3	3	239
Glyphorynchus spirurus	Understorey	13	11	11	11	11	11	11	11	337
Henicorhina leucosticta	Understorey	12	4	3	4	4	5	4	3	44
Lepidothrix coronata	Understorey	8	6	4	4	4	3	4	4	90
Microcerculus marginatus	Understorey	6	7	7	7	4	7	4	4	100
Myrmotherula axillaris	Understorey	6	3	3	3	3	3	2	2	230
Schiffornis turdina	Understorey	14	7	8	8	8	7	8	6	209
Sclerurus mexicanus	Understorey	7	6	5	6	7	4	9	3	63
Trogon rufus	Understorey	6	8	7	9	3	4	4	2	37
Xenops minutus	Understorey	10	8	8	9	8	8	8	8	218
	Average	9.45	6.55	6.18	6.45	5.64	5.55	5.45	4.45	157.55
	Std. Dev.	3.27	2.16	2.44	2.58	2.54	2.46	2.98	2.81	97.31

Supplementary Table 2 | Sensitivity analyses showing the impact of sample size on the number of species estimated in bGMYC. In each treatment the number of estimated bGMYC species using all samples was compared to the number of species estimated from data sets with a % of randomly pruned individuals. The number of observations was 27 for all tests. Shown are the *P* values for one and two-tailed tests.

Treatment	df	*t* value	*P* (one-tail)	*P* (two-tail)
10% pruned	51.1	0.4674	0.3211	0.6422
20% pruned	46.6	1.0179	0.157	0.314
30% pruned	43.7	1.4045	0.0836	0.1672
40% pruned	43.4	1.7173	0.0465	0.0931
50% pruned	45.1	1.8575	0.0349	0.0698
60% pruned	41.5	2.3803	0.0110	0.0220

Supplementary Table 3 | Lineages with a phylogeographic break across the Andes used to test simultaneous vicariance in hABC analysis, with samples sizes in each area and summary statistics scaled by per base-pair.

Population-pair	Sample Size (west/east)	π	θ_W	πNET	δ
Attila spadiceus	45/40	0.00398	0.0074	0.00496	0.03052
Automolus ochrolaemus **A**	20/56	0.0198	0.01539	0.04071	0.04349
Automolus ochrolaemus **B**	8/24	0.01076	0.00944	0.02262	0.02925
Brotogeris	6/18	0.02082	0.01597	0.04414	0.03558
Chlorophanes spiza	3/45	0.00245	0.00928	0.00273	0.03141
Colonia colonus	5/3	0.02552	0.02415	0.03349	0.02735
Cymbilaimus lineatus	9/7	0.00703	0.00713	0.00638	0.02089
Dendrocincla fuliginosa	17/38	0.01394	0.01165	0.02332	0.03482
Glyphorynchus spirurus	28/9	0.00628	0.00951	0.00405	0.03029
Henicorhina leucosticta	4/9	0.02183	0.0179	0.02743	0.03064
Lepidothrix coronata	13/7	0.02197	0.01528	0.03668	0.03303
Microcerculus marginatus	3/18	0.01114	0.01339	0.02386	0.03135
Myrmotherula axillaris	24/26	0.00911	0.00899	0.00917	0.03112
Piaya cayana	17/20	0.01505	0.01033	0.02525	0.03139
Pteroglossus	2/3	0.04183	0.03714	0.0355	0.02149
Pyrilia **A**	2/3	0.03943	0.03294	0.06038	0.02018
Pyrilia **B**	3/6	0.04058	0.03397	0.06874	0.03523
Pyrrhura **A**	3/7	0.01014	0.00796	0.00827	0.01790
Pyrrhura **B**	2/13	0.00622	0.00874	0.01218	0.02260
Querula purpurata	9/39	0.00541	0.00631	0.00703	0.02586
Schiffornis turdina **A**	11/17	0.02535	0.01683	0.04547	0.03799

Schiffornis turdina **B**	30/8	0.01052	0.00907	0.02461	0.02972
Sclerurus mexicanus	7/10	0.02487	0.01762	0.04265	0.03370
Tangara cyanicollis	12/13	0.0102	0.00691	0.01705	0.02357
Tangara gyrola	13/21	0.00596	0.00973	0.01424	0.02705
Tersina viridis	2/20	0.02138	0.01395	0.03805	0.03611
Tityra semifasciata	3/18	0.0036	0.00553	0.00861	0.02008
Trogon rufus	13/7	0.03154	0.02013	0.06064	0.03799
Xenops minutus	13/14	0.03593	0.02216	0.06271	0.04330

π = average pairwise genetic distance among DNA sequences sampled

θ_W = the number of segregating sites normalized for sample size

πNET = net average pairwise differences between populations

δ =the denominator of equation 38 in Tajima[72], where *S*, the number of segregating sites is scaled per base-pair rather than per locus

Phylogenetic position of A and B taxa are shown on corresponding gene trees

Supplementary Table 4 | Lineages with a phylogeographic break across the Isthmus of Panama used to test simultaneous vicariance, with samples sizes in each area and summary statistics scaled by per base-pair.

Population-pair	Sample Size (Central America/ Chocó)	π	θ_W	πNET	δ
Brotogeris	3/6*	0.0213	0.0165	0.0401	0.02430
Henicorhina leucosticta	8/7	0.1269	0.2284	0.0683	0.12595
Glyphorynchus spirurus	20/5	0.0036	0.0030	0.0077	0.01919
Lepidothrix coronata	5/8	0.0040	0.0040	0.0032	0.01431
Microcerculus marginatus	3/11	0.0185	0.0174	0.0475	0.03110
Myrmotherula axillaris	10/8	0.0024	0.0032	0.0018	0.01459
Pyrrhura	2/2	0.0142	0.0118	0.0206	0.00787
Querula purpurata	4/4	0.0008	0.0006	0.0015	0.00414
Schiffornis turdina	6/24	0.0021	0.0033	0.0028	0.01703
Sclerurus mexicanus	6/13	0.0459	0.0321	0.0944	0.04742
Tangara gyrola	13/19	0.0037	0.0055	0.0040	0.02219
Tityra semifasciata	3/27	0.0040	0.0053	0.0140	0.02149
Trogon rufus	2/13	0.0158	0.0190	0.0534	0.03346
Xenops minutus	27/14	0.0164	0.0107	0.0231	0.03277

* Samples are from the Tumbes region

π = average pairwise genetic distance among DNA sequences sampled

θ_W = the number of segregating sites normalized for sample size

πNET = net average pairwise differences between populations

δ = the denominator of equation 38 in Tajima[72], where *S*, the number of segregating sites is scaled per base-pair rather than per locus

Supplementary Table 5 | Lineages with a phylogeographic break across the Amazon River used to test simultaneous vicariance, with samples sizes in each area and summary statistics scaled by per base-pair.

Taxon-pair	Sample Size (Napo/ Inambari)	π	θ_W	πNET	δ
Brotogeris	4/4	0.00523	0.00395	0.00792	0.01095
Chlorophanes spiza	12/7	0.00224	0.00559	0.00013	0.01960
Cyanerpes caeruleus	4/5	0.00503	0.00574	0.00156	0.01428
Cymbilaimus lineatus	6/13	0.01111	0.01254	0.00236	0.02943
Dendrocicnla fuliginosa	6/7	0.02861	0.01814	0.05143	0.03085
Glyphorynchus spirurus	6/35	0.01847	0.01941	0.04943	0.04449
Lepidothrix coronata	19/37	0.02153	0.01881	0.02203	0.04602
Querula purpurata	4/11	0.00235	0.00271	0.00400	0.01256
Schiffornis turdina	13/16	0.01181	0.01061	0.01647	0.03035
Sclerurus mexicanus	5/8	0.00886	0.00631	0.01426	0.01809
Tangara gyrola	4/16	0.00479	0.00696	0.00041	0.02222
Tersina viridis	2/7	0.00405	0.00507	0.00109	0.01341
Trogon rufus	4/5	0.01639	0.01607	0.01273	0.02400
Xenops minutus	14/34	0.00885	0.01133	0.00856	0.03472

π = average pairwise genetic distance among DNA sequences sampled

θ_W = the number of segregating sites normalized for sample size

πNET = net average pairwise differences between populations

δ = the denominator of equation 38 in Tajima[72], where *S*, the number of segregating sites is scaled per base-pair rather than per locus

Phylogenetic position of A and B taxa are shown on corresponding gene trees

Supplementary Table 6 | Lineages with a phylogeographic break across the Negro River used to test simultaneous vicariance, with samples sizes in each area and summary statistics scaled by per base-pair.

Taxon-pair	Sample Size (Napo/Guiana)	π	θ_W	πNET	δ
Attila spadiceus	13/2	0.00104	0.00210	0.00007	0.01104
Automolus ochrolaemus	5/7	0.00308	0.00301	0.00113	0.01204
Brotogeris	4/18	0.00820	0.00868	0.01454	0.02555
Chlorophanes spiza	10/18	0.00174	0.00498	0.00005	0.02075
Colonia colonus	2/2	0.05339	0.05488	0.00000	0.01763
Cyanerpes caeruleus	4/18	0.00660	0.00943	0.00201	0.02663
Cymbilaimus lineatus	3/4	0.01459	0.01084	0.02435	0.01642
Dendrocincla fuliginosa	7/2	0.00073	0.00122	0.00022	0.00655

Glyphorynchus spirurus	34/106	0.02561	0.02794	0.04490	0.06319
Henicorhina leucosticta	9/15	0.01888	0.01514	0.02917	0.03464
Lepidothrix coronata	22/5	0.02491	0.02158	0.02183	0.04271
Pyrrhura	2/3	0.00078	0.00094	0.00049	0.00333
Querula purpurata	11/11	0.00387	0.00404	0.00233	0.01739
Schiffornis turdina	6/65	0.01574	0.03083	0.08922	0.06128
Sclerurus mexicanus	4/9	0.01610	0.01218	0.03237	0.02522
Tersina viridis	2/4	0.00381	0.00431	0.00081	0.00893
Trogon rufus	4/7	0.01462	0.01347	0.02049	0.02454

π = average pairwise genetic distance among DNA sequences sampled

θ_W = the number of segregating sites normalized for sample size

πNET = net average pairwise differences between populations

δ = the denominator of equation 38 in Tajima[72], where *S*, the number of segregating sites is scaled per base-pair rather than per locus

Supplementary Table 7 | Lineages with a phylogeographic break across the Madeira River used to test simultaneous vicariance, with samples sizes in each area and summary statistics scaled by per base-pair.

Taxon-pair	Sample Size (Inambari/ Rondônia)	π	θ_W	π_{NET}	δ
Attila spadiceus	17/8	0.00109	0.00310	0.00023	0.01577
Automolus ochrolaemus	45/23	0.00998	0.01135	0.01588	0.03672
Chlorophanes spiza	8/5	0.00256	0.00469	0.00024	0.01558
Cyanerpes caeruleus	6/4	0.01793	0.02973	0.00729	0.03496
Dendrocincla fuliginosa	23/32	0.02659	0.01803	0.00455	0.04492
Glyphorynchus spirurus	8/11	0.02913	0.02124	0.05489	0.03226
Microcerculus marginatus	21/10	0.01067	0.00818	0.01858	0.02703
Piaya cayana	8/11	0.00654	0.00966	0.00624	0.02580
Pyrilia	2/3	0.00948	0.01011	0.00849	0.01101
Pyrrhura	2/2	0.02775	0.02511	0.02840	0.01164
Schiffornis turdina	16/34	0.01615	0.01143	0.03291	0.03512
Tangara gyrola	16/4	0.00716	0.00843	0.00827	0.02447
Tersina viridis	6/7	0.00323	0.00413	0.00021	0.01462
Tityra semifasciata	11/4	0.00129	0.00245	0.00035	0.01192

π = average pairwise genetic distance among DNA sequences sampled

θ_W = the number of segregating sites normalized for sample size

πNET = net average pairwise differences between populations

δ = the denominator of equation 38 in Tajima[72], where *S*, the number of segregating sites is scaled per base-pair rather than per locus

Supplementary Table 8 | Phylogenetic generalized least-squares analyses (PGLS) parameters used to examine divergence levels and number of species in Neotropical forest birds.

Model	Response variable	Predictor variables in full model
	divergence levels	
m_1	Cross-Andes divergence times (n= 33)	ancestral origin, foraging stratum, niche breadth, lineage age
m_2	Cross-Isthmus of Panama divergence times (n = 18; n = 21)	ancestral origin, foraging stratum, niche breadth, lineage age
m_3	Cross-Amazonian Rivers divergence times (n = 31; n = 48)	ancestral origin, foraging stratum, niche breadth, lineage age, river,
	number of species	
m_4	Species diversity (n = 27)	ancestral origin, foraging stratum, niche breadth, lineage age

Shown are the response and predictor variables for the full phylogenetic generalized least-squares analyses (m_1 – m_4) used to examine divergence levels and number of species for the 27 bird lineages. Models m_1 – m_3 assessed the relationship between predictor variables and divergence times extracted from the time-calibrated gene trees. We accounted for the statistical non-independence of data by including a phylogenetic correction in each model. Divergence times across each barrier were modeled independently: m_1 – cross-Andes divergence levels, m_2 – cross-Isthmus of Panama divergence levels, and m_3 – cross-Amazonian river divergence levels. n_1 = sample size excluding 0 divergence times; n_2 sample size including 0 divergence times. Model m_4 examined the relationship between predictor variables and species diversity. The number of species in each of the 27 lineages was inferred by a coalescent-based Bayesian species delimitation method[59] as the overall total number of species or described taxa within each lineage (m_4). A complete description of each predictor variable is available in the *Ecological and historical variables* section of the Methods.

Supplementary Table 9 | Phylogenetic generalized least-squares analyses examining the effects of historical and ecological variables on divergence times across the Andes.

a) Results from univariate models

Effect	Estimate	Standard Error	*t* value	*P*	AICc
Lineage Age	0.3917	0.2325	1.6848	0.1021	74.5852
Foraging Stratum	0.0956	0.2728	0.3504	0.7284	77.3460
Ancestral Origin	0.2776	0.2595	1.0699	0.2929	76.3235
Niche Breadth	0.1022	1.3470	0.0759	0.9400	77.4704

Output of each univariate model: Lineage Age - Adjusted R^2: 0.0543; $f_{(df)}$: 2.839 $_{(1, 31)}$; P = 0.1021; n= 33. Foraging Stratum - Adjusted R^2: -0.0282; $f_{(df)}$: 0.1228 $_{(1, 31)}$; P = 0.7284; n= 33. Ancestral Origin - Adjusted R^2: 0.0045; $f_{(df)}$: 1.145 $_{(1, 31)}$; P = 0.2929; n= 33. Niche Breadth - Adjusted R^2: -0.0321; $f_{(df)}$: 0.0056 $_{(1, 31)}$; P = 0.94; n= 33.

b) Result from multivariate model

Effect	Estimate	Standard Error	*t* value	*P*
(Intercept)	-0.6887	0.8507	-0.8095	0.4250
Lineage Age	0.4727	0.2531	1.8679	0.0723
Foraging Stratum	0.0326	0.2859	0.1141	0.9100
Ancestral Origin	0.4030	0.2766	1.4574	0.1561
Niche Breadth	0.1234	1.5321	0.0806	0.9364

Output is from full model and the Δ AICc refers to the change in AICc when each predictor variable was removed from the full model. Lineage age is in units of millions of years. Full model AICc = 79.7969; Adjusted R^2: 0.0327; $f_{(df)}$: 1.27 $_{(4, 28)}$; P = 0.3052; n= 33. Lambda ML - 0.0; lower bound - 0.00, P = 1; upper bound 1.00, P < 0.0001. Model output for Foraging Stratum and Ancestral Origin correspond to the comparison of the reference level (Foraging Stratum – Understorey; Ancestral Origin East of the Andes) for each categorical variable

Supplementary Table 10 | Phylogenetic generalized least-squares analyses examining the effect of historical and ecological variables on genetic divergence levels across the Isthmus of Panama.

a) Results from univariate models without zero divergence times

Effect	Estimate	Standard Error	*t* value	*P*	AICc
Lineage Age	1.0390	0.4045	2.5683	0.0206	49.6329
Foraging Stratum	0.3472	0.5097	0.6811	0.5056	55.1222
Ancestral Origin	1.1081	0.3665	3.0233	0.0081	47.5878
Niche Breadth	1.1731	2.3519	0.4988	0.6247	55.4418

Output of each univariate model: Lineage Age - Adjusted R^2: 0.2477; $f_{(df)}$: 6.596 $_{(2, 16)}$; P = 0.0008; n= 18. Foraging Stratum - Adjusted R^2: -0.0326; $f_{(df)}$: 0.4639 $_{(2, 16)}$; P = 0.637; n= 18. Ancestral Origin - Adjusted R^2: 0.3238; $f_{(df)}$: 9.14 $_{(2, 16)}$; P = 0.0023; n= 18. Niche Breadth - Adjusted R^2: -0.0462; $f_{(df)}$: 0.2488 $_{(2, 16)}$; P = 0.7827; n= 18.

b) Result from multivariate model without zero divergence times

Effect	Estimate	Standard Error	*t* value	*P*
(Intercept)	-3.5796	0.8959	-3.9954	0.0015
Lineage Age	1.1162	0.2893	3.8587	0.0020
Foraging Stratum	0.1021	0.3249	0.3143	0.7583
Ancestral Origin	1.3669	0.2839	4.6514	0.0005
Niche Breadth	1.7687	1.5694	1.1270	0.2801

c) Result from multivariate model with zero divergence times included

Effect	Estimate	Standard Error	*t* value	*P*
(Intercept)	-4.6611	1.3823	-3.3720	0.0039
Lineage Age	1.3039	0.4023	3.2408	0.0051
Foraging Stratum	0.5756	0.4647	1.2385	0.2334
Ancestral Origin	1.0317	0.4016	2.5694	0.0206
Niche Breadth	2.8832	2.2276	1.2943	0.2139

Output is from full model and the Δ AICc refers to the change in AICc when each predictor variable was removed from the full model. Lineage age is in units of millions of years. a) Full model (without zero divergences) AICc =42.1344; Adjusted R^2: 0.6563; $f_{(df)}$: 9.019 $_{(5, 13)}$; P = 0.0007; n= 18. Lambda ML - 0.0; lower bound - 0.00, P = 1; upper bound 1.00, P = 0.0038. b) Full model (with zero divergences) AICc = 64.0856; Adjusted R^2: 0.4344; $f_{(df)}$: 4.84$_{(5, 16)}$; P = 0.0129; n= 21. Lambda ML - 0.330; lower bound - 0.00, P = 0.4672; upper bound 1.00, P = 0.1007. Model output for Foraging Stratum and Ancestral Origin correspond to the comparison of the reference level (Foraging Stratum – Understorey; Ancestral Origin East of the Andes) for each categorical variable.

Supplementary Table 11 | Phylogenetic generalized least-squares analyses examining the effect of historical and ecological variables on divergence times across Amazonian rivers.

a) Results from univariate models without zero divergence times.

Effect	Estimate	Standard Error	*t* value	*P*	AICc
Lineage Age	0.2460	0.3070	0.8013	0.4295	68.7123
Foraging Stratum	0.8994	0.2305	3.902	0.0005	58.6586
Ancestral Origin	-0.5985	0.2569	-2.3296	0.027	64.0406
River - Negro	0.2994	0.2395	1.2502	0.2216	67.8280
River - Amazon	-0.2145	0.2660	-0.8062	0.4269	
Niche Breadth	-1.2053	1.5704	-0.7675	0.449	68.7740

Output of each univariate model: Lineage Age - Adjusted R^2: -0.0121; $f_{(df)}$: 0.6421 $_{(1, 29)}$; P = 0.4295; n= 33. Foraging Stratum - Adjusted R^2: 0.3217; $f_{(df)}$: 15.23 $_{(1, 29)}$; P = 0.0005; n= 33. Ancestral Origin - Adjusted R^2: 0.1286; $f_{(df)}$: 5.427 $_{(1, 29)}$; P = 0.027; n= 33. River - Adjusted R^2: 0.1; $f_{(df)}$: 2.668 $_{(2, 28)}$; P = 0.0870; n= 33. Niche Breadth - Adjusted R^2: -0.0139; $f_{(df)}$: 0.5891 $_{(1, 29)}$; P = 0.449; n= 33.

b) Result from multivariate model without zero divergence times

Effect	Estimate	Standard Error	*t* value	*P*
(Intercept)	0.4330	0.7227	0.5992	0.5547
Lineage Age	0.1347	0.2103	0.6404	0.5280
Foraging Stratum	0.7926	0.2028	3.9087	0.0007
Ancestral Origin	-0.6898	0.2046	-3.3714	0.0025
River - Negro	0.1027	0.2293	0.4479	0.6582
River - Amazon	-0.4627	0.2616	-1.7687	0.0897
Niche Breadth	-1.4871	1.1693	-1.2718	0.2156

c) Result from multivariate model with zero divergence times

Effect	Estimate	Standard Error	*t* value	*P*
(Intercept)	-0.7686	1.1297	-0.6804	0.5001
Lineage Age	0.6734	0.2782	2.4211	0.0200
Foraging Stratum	1.4317	0.2861	5.0048	<0.0001
Ancestral Origin	-0.2812	0.3115	-0.9029	0.3719
River - Negro	0.2200	0.3246	0.6777	0.5018
River - Amazon	-0.5625	0.3342	-1.6833	0.0999
Niche	-3.3690	1.7869	-1.8854	0.0665

Output is from full model and the Δ AICc refers to the change in AICc when each predictor variable was removed from the full model. Lineage age is in units of millions of years. b) Full model (without zero divergences) AICc = 57.0086; Adjusted R^2: 0.5122; $f_{(df)}$: 6.251 $_{(6, 24)}$; P = 0.0005; n= 31. Lambda ML - 0.0; lower bound - 0.00, P = 1; upper bound 1.00, P < 0.0001. c) Full model (with zero divergences) AICc = 132.8105; Adjusted R^2: 0.5536; $f_{(df)}$: 10.71 $_{(6, 41)}$; P < 0.0001; n= 48. Lambda ML - 0.0; lower bound - 0.00, P = 1; upper bound 1.00, P < 0.0001. Model output for Foraging Stratum, Ancestral

Origin, and River correspond to the comparison of the reference level (Foraging Stratum – Understorey; Ancestral Origin – East of the Andes; River – Madeira) for each categorical variable.

Supplementary Table 12 | Univariate phylogenetic generalized least-squares analyses examining the effects of historical and ecological variables on species diversity.

Effect	Estimate	Standard Error	*t* value	*P*	AICc
Lineage Crown Age	0.2477	0.0599	4.1322	0.0004	48.4397
Lineage Stem Age	0.1426	0.0292	4.8861	<0.0001	44.3954
Foraging Stratum	0.6357	0.2701	2.3539	0.0267	50.8017
Ancestral Origin	-0.5031	0.2059	-2.4435	0.0219	50.549
Niche Breadth	-0.0793	1.2631	-0.0628	0.9504	56.1602

Output of each univariate model: Lineage Crown Age - Adjusted R^2 0.3821; $F_{s\,(df)}$: 17.08 $_{(1, 25)}$; P = 0.0004; n= 27. Lineage Stem Age - Adjusted R^2: 0.468; $f_{(df)}$: 23.87 $_{(1, 25)}$; P = 5.005e-05; n= 27. Foraging Stratum - Adjusted R^2: 0.1487; $f_{(df)}$: 5.541 $_{(1, 25)}$; P = 0.0267; n= 27. Ancestral Origin - Adjusted R^2: 0.1605; $f_{(df)}$: 5.971 $_{(1, 25)}$; P = 0.0219; n= 27. Niche Breadth - Adjusted R^2: -0.0398; $f_{(df)}$: 0.0040 $_{(1, 25)}$; P = 0.9504; n= 27. Lineage age is in units of millions of years.

Supplementary Table 13 | Relative importance of each predictor variable determined with Δ AICc values from the phylogenetic generalized least-squares analyses assessing divergences across the Andes.

	Ancestral Origin	Foraging Stratum	Niche Breadth	Lineage Age
Δ AICc A	-0.3809	-2.7783	-2.7860	1.0816
Δ AICc B	-1.1886	-2.2094	-2.7915	-0.3745
Δ AICc C	1.8880	-2.7621	-2.2287	-0.0987

Shown are models using cross Andes divergences as the response variable. Variable importance was measured by Δ AICc, which is the change in AICc when the predictor variable is removed from the full model. Δ AIC values > 2 are considered significant. Reported are Δ AICc scores in which mean (Δ AICc A), low (Δ AICc B) or high (Δ AICc C) 95% HPD cross Andes divergence was used. AICc scores for full models using mean, the low 95% HPD, and the high 95% HPD, respectively: 79.7969, 92.0685, 76.9737. Lineage Age is stem age.

Supplementary Table 14 | Relative importance of each predictor variable determined with Δ AICc values from the phylogenetic generalized least-squares analyses assessing divergences across the Isthmus of Panama.

a) Model comparisons without zero divergence times

	Ancestral Origin	Foraging Stratum	Niche Breadth	Lineage Age
Δ AICc A	13.7156	-3.7868	-2.2451	8.5055
Δ AICc B	13.5445	-3.7363	-2.6658	8.2753
Δ AICc C	13.3236	-3.8180	-2.1881	8.1927

b) Model comparisons with zero divergence times included

	Ancestral Origin	Foraging Stratum	Niche Breadth	Stem Age
Δ AICc A	3.7433	-2.0258	-1.4744	6.4914
Δ AICc B	8.8970	-1.7535	-1.2001	7.4605
Δ AICc C	1.2274	-2.2250	-1.8434	5.4432

Shown are models using cross Andes divergences as the response variable. Variable importance was measured by Δ AICc, which is the change in AICc when the predictor variable is removed from the full model. Δ AIC values > 2 are considered significant. Reported are Δ AICc scores in which mean (Δ AICc A), low (Δ AICc B) or high (Δ AICc C) 95% HPD cross Andes divergence was used. AICc scores for full models using mean, the low 95% HPD, and the high 95% HPD, respectively: a) Full model without zero divergence times: 42.1344, 48.0538, 40.2236; b) Full model with zero divergence times: 64.0856, 59.8406, 68.9057. Lineage Age is stem age.

Supplementary Table 15 | Relative importance of each predictor variable determined with Δ AICc values from the phylogenetic generalized least-squares analyses assessing divergences across Amazonian rivers.

a) Model comparisons without zero divergence times

	Ancestral Origin	Foraging Stratum	Niche Breadth	Stem Age	River
Δ AICc A	8.6493	9.4058	-1.3476	-2.8443	0.5731
Δ AICc B	9.6711	10.0460	-1.2158	-3.0597	-0.5047
Δ AICc C	8.0215	8.2501	-1.3890	-2.7984	1.5659

b) Model comparisons with zero divergence times included

	Ancestral Origin	Foraging Stratum	Niche Breadth	Stem Age	River
Δ AICc A	-1.8062	9.3190	1.2398	2.9226	1.7316
Δ AICc B	0.5782	13.4094	1.5677	1.1055	2.6313
Δ AICc C	-2.4823	7.7313	1.0098	3.8067	1.4867

Shown are models using cross Andes divergences as the response variable. Variable importance was measured by Δ AICc, which is the change in AICc when the predictor variable is removed from the full model. Δ AIC values > 2 are considered significant. Reported are Δ AICc scores in which mean (Δ AICc A), low (Δ AICc B) or high (Δ AICc C) 95% HPD cross Andes divergence was used. AICc scores for full models using mean, the low 95% HPD, and the high 95% HPD,

respectively: a) Full model without zero divergence times: 57.0086, 67.5593, 51.5928; b) Full model with zero divergence times: 133.5591, 117.0998, 145.3611. Lineage Age is stem age.

Supplementary Table 16 | Relative importance of each predictor variable determined with Δ AIC values from the phylogenetic generalized least-squares analyses assessing diversity.

Data set	Δ AIC	Ancestral Origin	Foraging Stratum	Niche Breadth	Stem Age
Full	Δ AICc A	-1.9546	4.0122	-1.9595	6.9586
	Δ AICc B	-1.6645	2.8719	-1.6710	12.1708
	Δ AICc C	-2.2471	4.1784	-2.6307	3.0659
10% pruned	Δ AICc A	-2.3370	3.8452	-0.7117	6.0261
	Δ AICc B	-2.1630	2.6436	-0.2495	9.9617
	Δ AICc C	-2.5318	4.3561	-1.3133	2.5947
20% pruned	Δ AICc A	-2.9949	14.7324	-0.8372	5.9602
	Δ AICc B	-2.9914	13.9077	-0.5571	8.8632
	Δ AICc C	-2.9368	16.1837	-0.6135	5.2660
30% pruned	Δ AICc A	-2.2903	7.8654	0.5107	3.7659
	Δ AICc B	-2.2162	7.0030	0.8195	5.7766
	Δ AICc C	-2.4034	7.1533	0.9896	2.1080
40% pruned	Δ AICc A	-2.8091	11.1890	-0.3828	-1.0755
	Δ AICc B	-2.8206	10.3410	-0.3256	-0.1421
	Δ AICc C	-2.8683	11.9767	-0.2610	-1.0967
50% pruned	Δ AICc A	-3.0389	9.9027	-0.1020	0.3388
	Δ AICc B	-3.0389	8.5128	0.0265	1.6970
	Δ AICc C	-3.0290	10.9465	0.0494	0.7021
60% pruned	Δ AICc A	-2.0499	1.9926	-2.1203	-0.8841
	Δ AICc B	-2.0244	1.3488	-2.0945	-0.1799
	Δ AICc C	-2.2160	2.7264	-2.0592	-0.7147

Shown are models using either bGMYC species from all the samples (full) and the randomly pruned bGMYC species data sets (10%-60%). Variable importance was measured by Δ AIC, which is the change in AIC when the predictor variable is removed from the full model. Δ AIC values > 2 are considered significant. Reported are Δ AIC scores in which mean (Δ AICc A), low (Δ AICc B) or high (Δ AICc C)

95% HPD stem age was used as the predictor variable. AIC scores for full models using mean, the low 95% HPD, and the high 95% HPD, respectively: *Full*: 43.7365, 38.5242, 47.6291; *10% Pruned:* 42.7542, 38.8186, 46.1856; *20% pruned*: 33.5380, 30.6350, 34.2322; *30% pruned:* 31.9908, 29.9802, 33.6487 ;

40% pruned: 36.1306, 35.1972, 36.1517; *50% pruned*: 38.8414, 37.4833, 38.4782; *60% pruned:* 38.3087, 37.6046, 38.1394

.

References

31. Weckstein, J.D. Molecular phylogenetics of the *Ramphastos* toucans: implications for the evolution of morphology, vocalizations, and coloration. *Auk,* **122**, 1191-1209 (2005).
32. Patané, J.S., Weckstein, J.D., Aleixo, A. & Bates, J.M. Evolutionary history of *Ramphastos* toucans: Molecular phylogenetics, temporal diversification, and biogeography. *Mol. Phylogen. Evol.,* **53**, 923-934 (2009).
33. Patel, S., Weckstein, J.D., Patané, J.S.L., Bates, J.M. & Aleixo, A. Temporal and spatial diversification of *Pteroglossus* araçaris (Aves: Ramphastidae) in the Neotropics: constant rate of diversification does not support a Pleistocene radiation. *Mol. Phylogen. Evol*., **58**, 105–115 (2011).
34. Ribas, C.C., Joseph L. & Miyaki C.Y. Molecular systematics and patterns of diversification of the *Pyrrhura* parakeets (Aves: Psittacidae) with special reference to the *P. picta* / *P. leucotis* complex. *Auk,* **123**, 660–680 (2006).
35. Ribas, C.C., Miyaki, C.Y. & Cracraft, J. Phylogenetic relationships, diversification and biogeography in Neotropical *Brotogeris* parakeets. *J. Biogeogr.,* **36**, 1712-1729 (2009).
36. Ribas, C.C., Miyaki, C.Y., Gaban-Lima, R. & Cracraft, J. Historical biogeography and diversification within the Neotropical parrot genus *Pionopsitta* (Aves: Psittacidae). *J. Biogeog.,* **32**, 1409–1427 (2005).
37. Barraclough, T. G., & Vogler, A. P. Detecting the geographical pattern of speciation from species-level phylogenies. Am, Nat., **155**, 419-434 (2000).
38. Edwards, S. V., Kingan, S. B., Calkins, J. D., Balakrishnan, C. N., Jennings, W. B et al. Speciation in birds: genes, geography, and sexual selection. Proc Natl Acad Sci., **102**, 6550-6557 (2005).
39. Price, T. *Speciation in birds*. Roberts and Company, Boulder, CO, USA (2008).
40. Simpson, B. B., & Haffer, J. Speciation patterns in the Amazonian forest biota. *Annu. Rev. Ecol. Evol. Syst.*, **9**, 497-518 (1978).
41. Sorenson, M. D., Ast, J. C., Dimcheff, D. E., Yuri, T., & Mindell, D. P. Primers for a PCR-based approach to mitochondrial genome sequencing in birds and other vertebrates. Mol. Phylogenet. Evol., **12**, 105–114 (1999).
42. McCormack, J.E. et al. Ultraconserved elements are novel phylogenomic markers that resolve placental mammal phylogeny when combined with species-tree analysis. *Genome Res.,* **22**, 746-754 (2012).
43. Faircloth, B.C. et al. Ultraconserved elements anchor thousands of genetic markers spanning multiple evolutionary timescales. *Syst. Biol.,* **61**, 717-726 (2012).
44. Crawford, N.G. et al., More than 1000 ultraconserved elements provide evidence that turtles are the sister group of archosaurs. *Biol. Lett.,* **8**, 783-786 (2012).
45. McCormack, J.E. et al., A phylogeny of birds based on over 1,500 loci collected by target enrichment and high-throughput sequencing. *PLoS ONE,* **8**, e54848 (2013).
46. Smith, B.T., Harvey, M.G., Faircloth, B.C., Glenn, T.C. & Brumfield, R.T. Target capture and massively parallel sequencing of ultraconserved elements (UCEs) for comparative studies at shallow time scales. *Syst. Biol.,* **63**, 83-95 (2014).
47. McCormack, J.E., Heled, J., Delaney, K.S., Peterson, A.T. & Knowles, L.L. Calibrating divergence times on species trees versus gene trees: implications for speciation history of *Aphelocoma* jays. *Evolution,* **65**,184-202 (2011).
48. Cracraft, J. Historical biogeography and patterns of differentiation within the South American avifauna: areas of endemism. *Ornithological Monographs* 49-84 (1985).
49. Haffer, J. Avian zoogeography of the Neotropical lowlands. *Ornithological Monographs*, 113-146 (1985).
50. A.J. Drummond, A. Rambaut, BEAST: Bayesian evolutionary analysis by sampling trees. *BMC Evol. Biol.,* **7**, 214 (2007).
51. Weir, J.T. & Schluter, D. Calibrating the avian molecular clock. *Mol. Ecol.,* **17**, 2321-2328 (2008).
52. Rambaut, A. & Drummond, A.J. *Tracer v 1.5.* (Distributed by the authors.

University of Oxford, Oxford 2010).
53. Smith, B.T. & Klicka, J. Examining the role of effective population size on mitochondrial and multilocus divergence time discordance in a songbird. *PLoS ONE,* **8**, e55161 (2013).
54. Smith, B.T., Ribas, C.C., Whitney, B.W., Hernández-Baños, B.E. & Klicka, J. Identifying biases at different spatial and temporal scales of diversification: a case study using the Neotropical parrotlet genus *Forpus*. *Mol. Ecol.,* **22**, 483-494 (2013).
55. Lemey, P., Rambaut, A., Drummond, A.J. & Suchard, M.A. Bayesian phylogeography finds its roots. *PLoS Comput. Biol.,* **5**, e1000520 (2009).
56. Tobias, J.A., Bates, J.M., Hackett, S.J. & Seddon, N. Comment on The Latitudinal Gradient in Recent Speciation and Extinction Rates of Birds and mammals. *Science,* 901c (2008).
57. Milá, B. et al. A trans-Amazonian screening of mtDNA reveals deep intraspecific divergence in forest birds and suggests a vast underestimation of species diversity. *PloS ONE*, **7**, e40541 (2012).
58. Dynesius, M. & Jansson, R. Persistence of within-species lineages: a neglected control of speciation rates. Evolution, **68**, 923-934 (2014).
59. Reid, N. & Carstens, B. Phylogenetic estimation error can decrease the accuracy of species delimitation: a Bayesian implementation of the general mixed Yule-coalescent model. *BMC Evol. Biol.,* **12**, 196 (2012).
60. Pons, J. et al. Sequence-based species delimitation for the DNA taxonomy of undescribed insects. *Syst. Biol.,* **55**, 595-609 (2006).
61. Paradis, E., Claude, J., & Strimmer, K. (2004). APE: analyses of phylogenetics and evolution in R language. *Bioinformatics*, **20**, 289-290.
62. Remsen, J. V., Jr., Cadena, C. D., Jaramillo, A., Nores, M., et al. A classification of the bird species of South America. American Ornithologists' Union. http://www.museum.lsu.edu/~Remsen/SACCbaesline.html (2014).
63. Huang, W., Takebayashi, N., Qi, Y. & Hickerson, M.J. MTML-msBayes: Approximate Bayesian comparative phylogeographic inference from multiple taxa and multiple loci with rate heterogeneity. *BMC Bioinformatics,* **12**, 1 (2011).
64. Beaumont, M.A., Zhang, W.Y. & Balding, D.J. Approximate Bayesian computation in population genetics. *Genetics,* **162**, 2025-2035 (2002).
65. Hickerson, M.J., Dolman, G. & Moritz, C. Phylogeographic summary statistics for testing simultaneous vicariance. *Mol. Ecol.,* **15**, 209-223 (2006).
66. Gelman, A., Carlin, J. B., Stern, H. S. & Rubin, D. B. *Bayesian data analysis* (Chapman and Hall/CRC, London 2004).
67. Beaumont, B. A. & Rannala, B. The Bayesian revolution in genetics. *Nat. Rev. Genet.,* **5**, 251-261 (2004).
68. Hickerson, M.J. et al. Recommendations for using msBayes to incorporate uncertainty in selecting an ABC model prior: A response to Oaks et al. Evolution, **68**, 284-294 (2014).
69. Oaks, J.R. et al. Evidence for climate-driven diversification? A caution for interpreting ABC inferences of simultaneous historical events. *Evolution,* **67**, 991-1010 (2013).
70. Cornuet, J. M., Ravigné, V. & Estoup, A. Inference on population history and model checking using DNA sequence and microsatellite data with the software DIYABC (v1. 0). *BMC Bioinformatics,* **11**, 401 (2010).
71. Jeffries, H. *The theory of probability* (Oxford, Oxford University Press, 1961).
72. Tajima, F. Statistical method for testing the neutral mutation hypothesis by DNA polymorphism. Genetics, **123**, 585-595 (1989).
73. Parker III, T. A., Stotz, D. F. & Fitzpatrick, J. W. *Ecological and distributional databases*, (Eds. Stotz, D. F., Fitzpatrick, J. W., Parker III, T. A. & Moskovits, D.K. University of Chicago Press, Chicago, 1996).
74. Ricklefs, R.E. Estimating diversification rates from phylogenetic information. *Trends Ecol. Evol.* **22**, 601-610 (2007).

75. Hijmans, R.J., Cameron, S.E., Parra, J.L., Jones, P.G. & Jarvis, A. Very high resolution interpolated climate surfaces for global land areas. *Int. J. Clim.,* **25**, 1965-1978 (2005).
76. Warren, D.L., Glor, R.E. & Turelli, M. ENMTools: a toolbox for comparative studies of environmental niche models. *Ecography,* **33**, 607-611 (2010).
77. Phillips, S. J., Dudík, M. & Schapire, R.E. Maxent software for species habitat modeling, version 3.3. 1. (2006).
78. Nakazato, T.,Warren, D.L. & Moyle, L.C. Ecological and geographic modes of species divergence in wild tomatoes. *Am. J. Bot.,* **97**, 680-693 (2010).
79. Cadena, C. D. et al. Latitude, elevational climatic zonation and speciation in New World vertebrates. Proceedings of the Royal Society B: Biological Sciences, 279, 194-201 (2012).
80. Salisbury, C.L, Seddon, N., Cooney, C.R. & Tobias, J.A. The latitudinal gradient in dispersal constraints: ecological specialisation drives diversification in tropical birds. *Ecol. Lett.,* **15**, 847-855 (2012).
81. Ridgely, R.S. et al., *Digital distribution maps of the birds of the western hemisphere*, v. 232 1.0. NatureServe, Arlington, Virginia, USA (2003).
82. Antonelli, A., Nylander, J. A., Persson, C. & Sanmartín, I. Tracing the impact of the Andean uplift on Neotropical plant evolution. *Proc. Natl Acad. Sci. USA,* **106**, 9749-9754 (2009).
83. Moore, B.R. & Donoghue, M.J. Correlates of diversification in the plant clade Dipsacales: geographic movement and evolutionary innovations. Am. Nat., **170**, S28-S55 (2007).
84. Orme, C. D. L., Freckleton, R. P., Thomas, G. H., Petzoldt, T., Fritz, S. A., Isaac, N., & Pearse, W. (2012). caper: comparative analyses of phylogenetics and evolution in R. R package version 0.5 (2012).
85. Team, R. C. R: A language and environment for statistical computing. R foundation for Statistical Computing (2012).
86. Bolker, B.M. et al. Generalized linear mixed models: a practical guide for ecology and evolution. *Trends Ecol. Evol.* **24**, 127-135 (2009).
87. Clements, J. F. et al. The eBird/Clements checklist of birds of the world: Version 6.8 (2013).

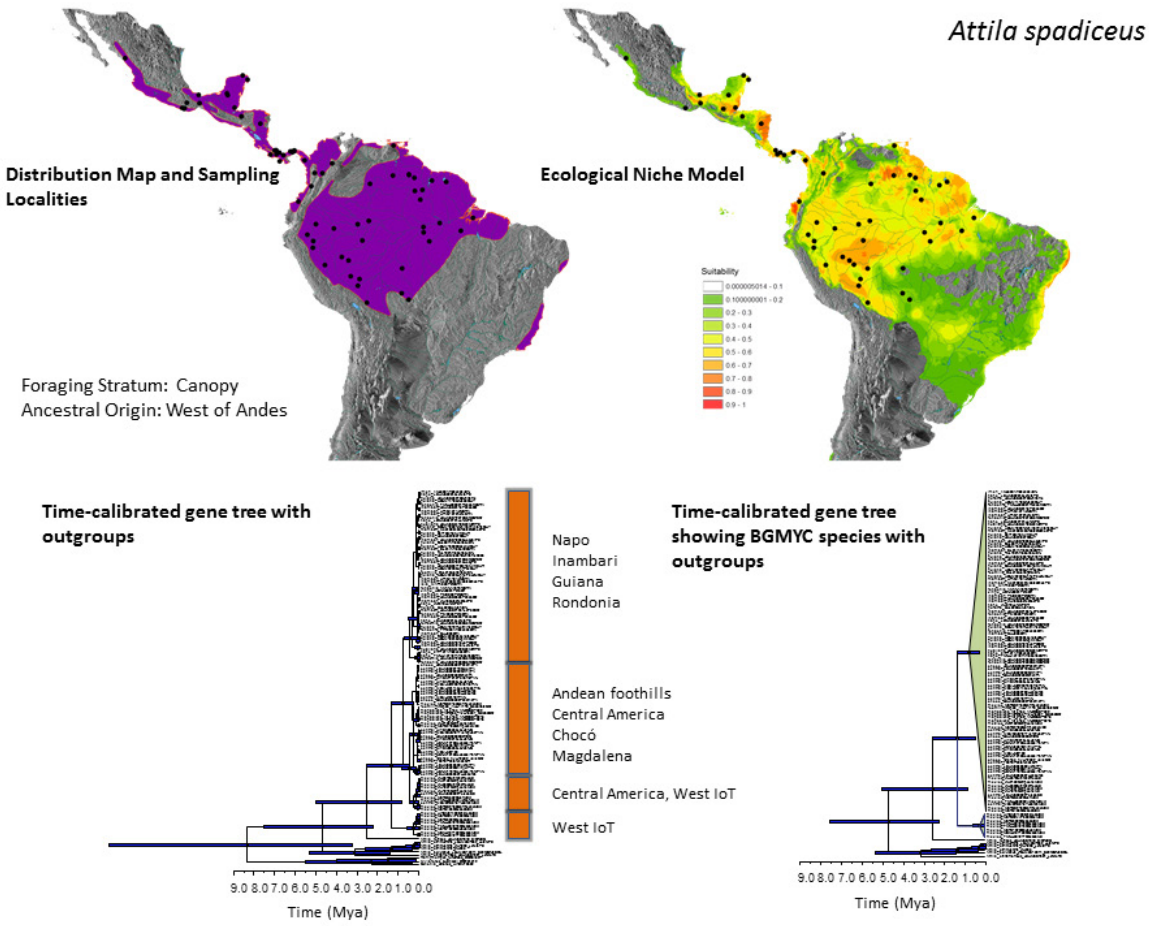

Supplementary Figure 1 | Range map, ENM, time-calibrated gene trees and delimited species for *Attila spadiceus.* Range map (natureserv.org) showing approximate geographic distribution of each lineage with sampling localities as black circles (upper left). Ecological niche model (ENM) indicating areas with suitable climatic conditions from 0 (clear) to 1.0 (red); locality records used to construct the ENM appear as black circles (upper right). Time-calibrated gene tree showing geographic clades (bottom left). Time-calibrated gene tree with clades collapsed to show species delimited using bGMYC (bottom right).

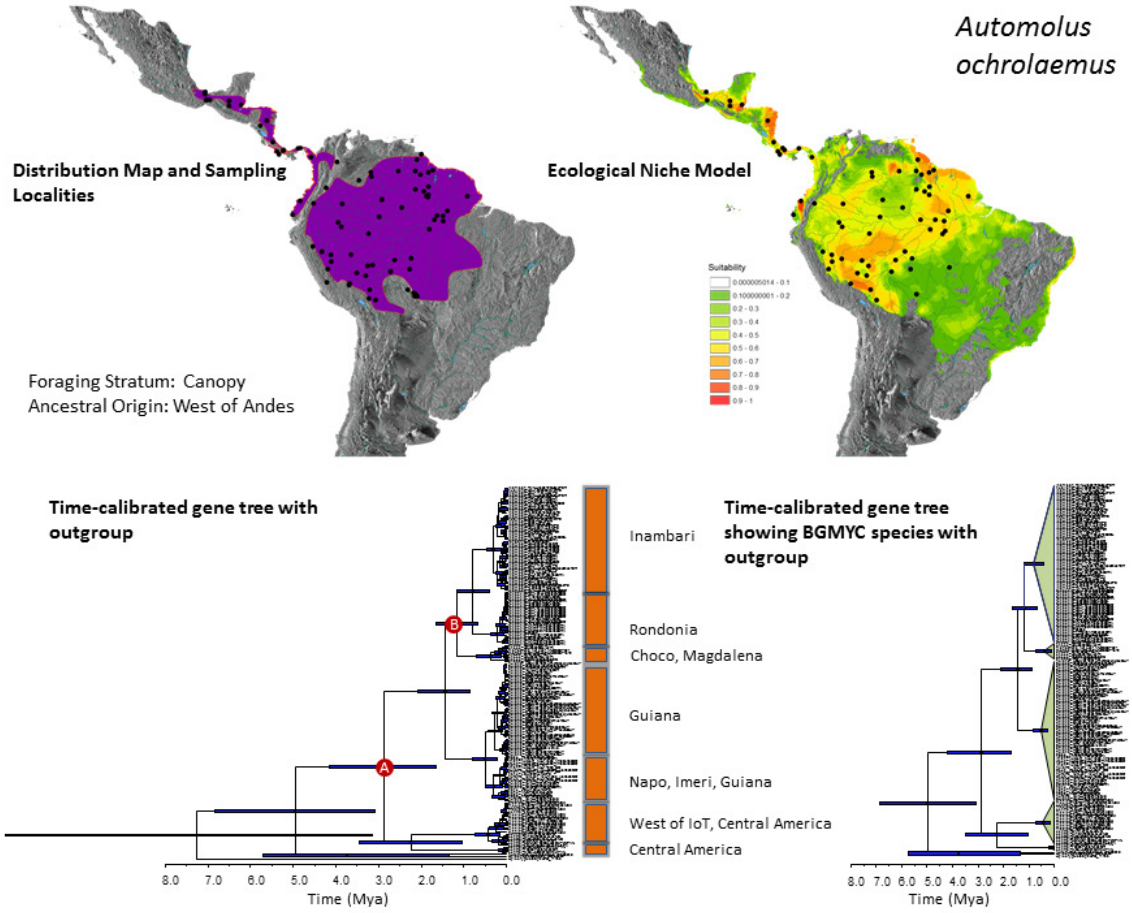

Supplementary Figure 2 | Range map, ENM, time-calibrated gene trees and delimited species for *Automolus ochrolaemus*. Range map (natureserv.org) showing approximate geographic distribution of each lineage with sampling localities as black circles (upper left). Ecological niche model (ENM) indicating areas with suitable climatic conditions from 0 (clear) to 1.0 (red); locality records used to construct the ENM appear as black circles (upper right). Time-calibrated gene tree showing geographic clades (bottom left). Time-calibrated gene tree with clades collapsed to show species delimited using bGMYC (bottom right). Nodes labeled A and B refer to multiple cross-Andes divergence events used in the msBayes analysis.

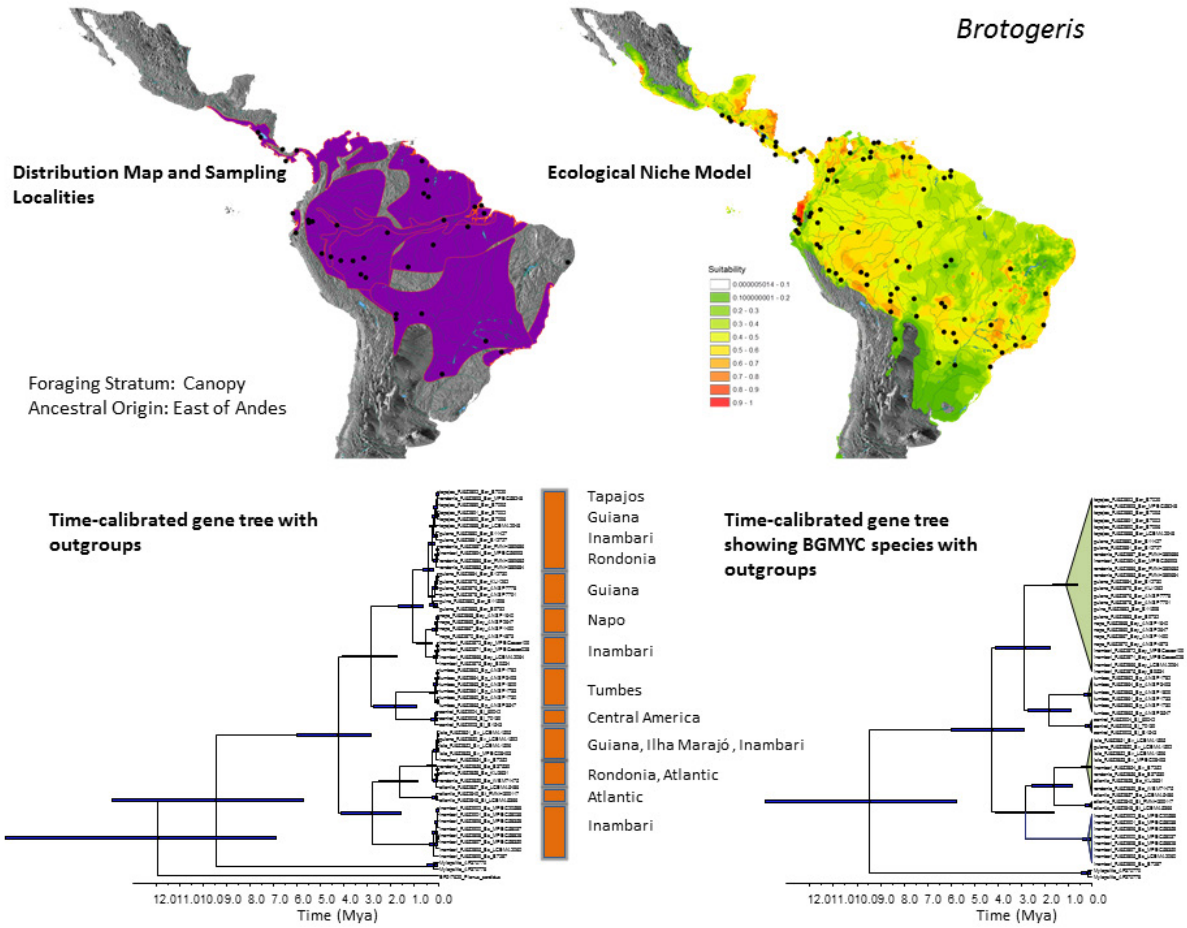

Supplementary Figure 3 | Range map, ENM, time-calibrated gene trees and delimited species for *Brotogeris*. Ingroup includes all biological species in *Brotogeris*: B. *tirica, B. versicolurus, B. chiriri, B. sanctithomae, B. pyrrhoptera, B. jugularis, B. cyanoptera,*and *B. chrysoptera.* Range map (natureserv.org) showing approximate geographic distribution of each lineage with sampling localities as black circles (upper left). Ecological niche model (ENM) indicating areas with suitable climatic conditions from 0 (clear) to 1.0 (red); locality records used to construct the ENM appear as black circles (upper right). Time-calibrated gene tree showing geographic clades (bottom left). Time-calibrated gene tree with clades collapsed to show species delimited using bGMYC (bottom right).

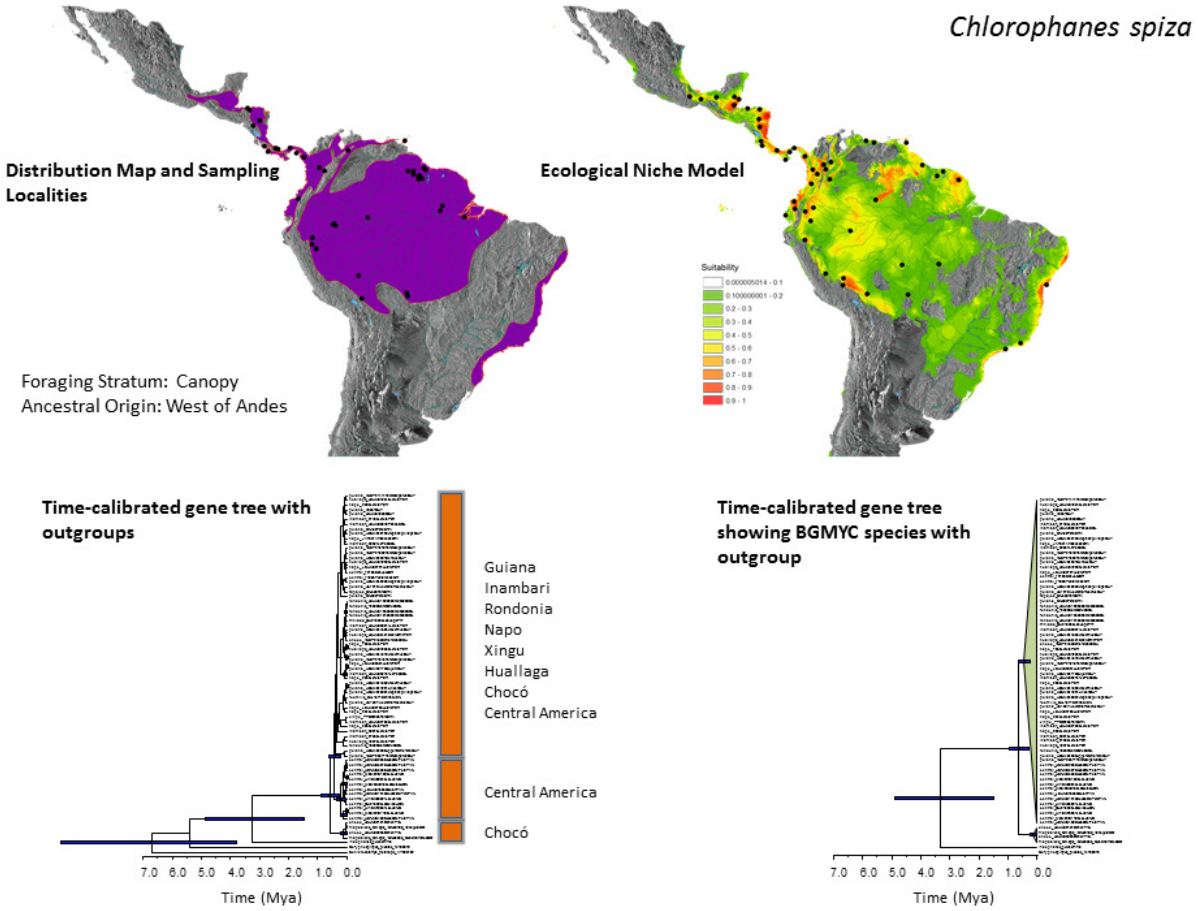

Supplementary Figure 4 | Range map, ENM, time-calibrated gene trees and delimited species for *Chlorophanes spiza.* Range map (natureserv.org) showing approximate geographic distribution of each lineage with sampling localities as black circles (upper left). Ecological niche model (ENM) indicating areas with suitable climatic conditions from 0 (clear) to 1.0 (red); locality records used to construct the ENM appear as black circles (upper right). Time-calibrated gene tree showing geographic clades (bottom left). Time-calibrated gene tree with clades collapsed to show species delimited using bGMYC (bottom right).

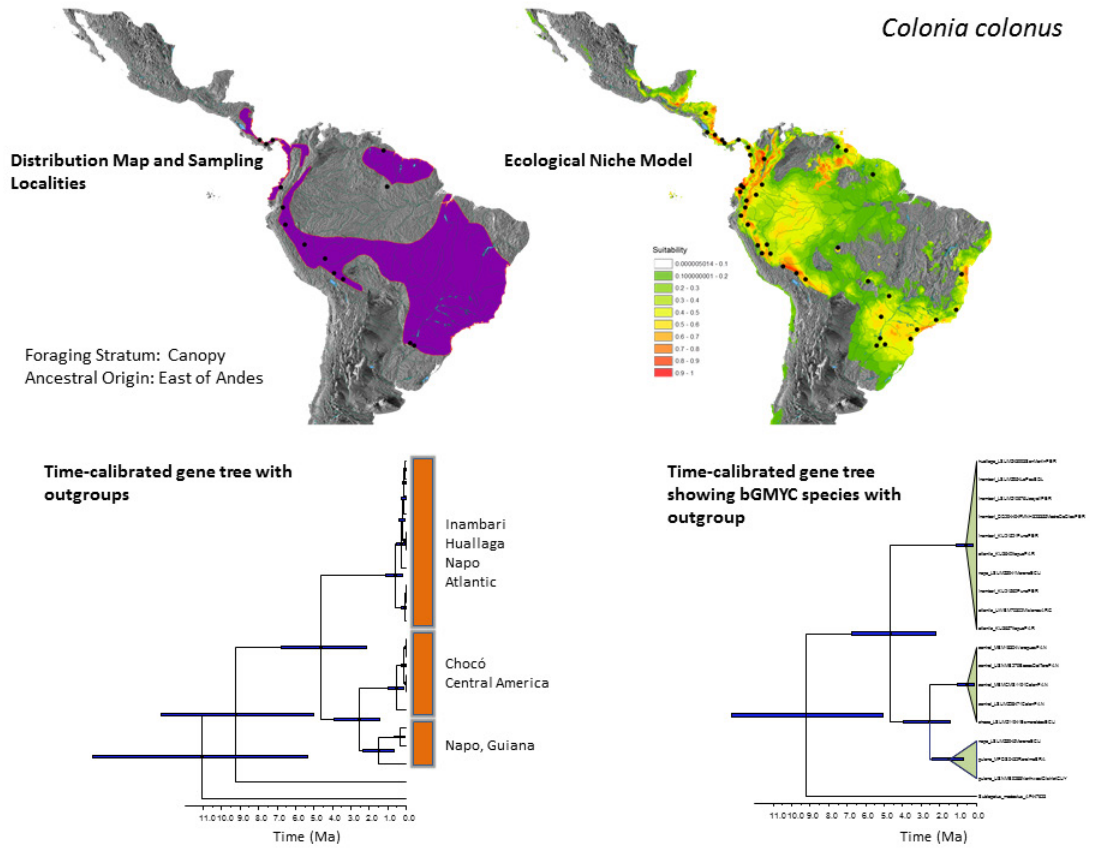

Supplementary Figure 5 | Range map, ENM, time-calibrated gene trees and delimited species for *Colonia colonus.* Range map (natureserv.org) showing approximate geographic distribution of each lineage with sampling localities as black circles (upper left). Ecological niche model (ENM) indicating areas with suitable climatic conditions from 0 (clear) to 1.0 (red); locality records used to construct the ENM appear as black circles (upper right). Time-calibrated gene tree showing geographic clades (bottom left). Time-calibrated gene tree with clades collapsed to show species delimited using bGMYC (bottom right).

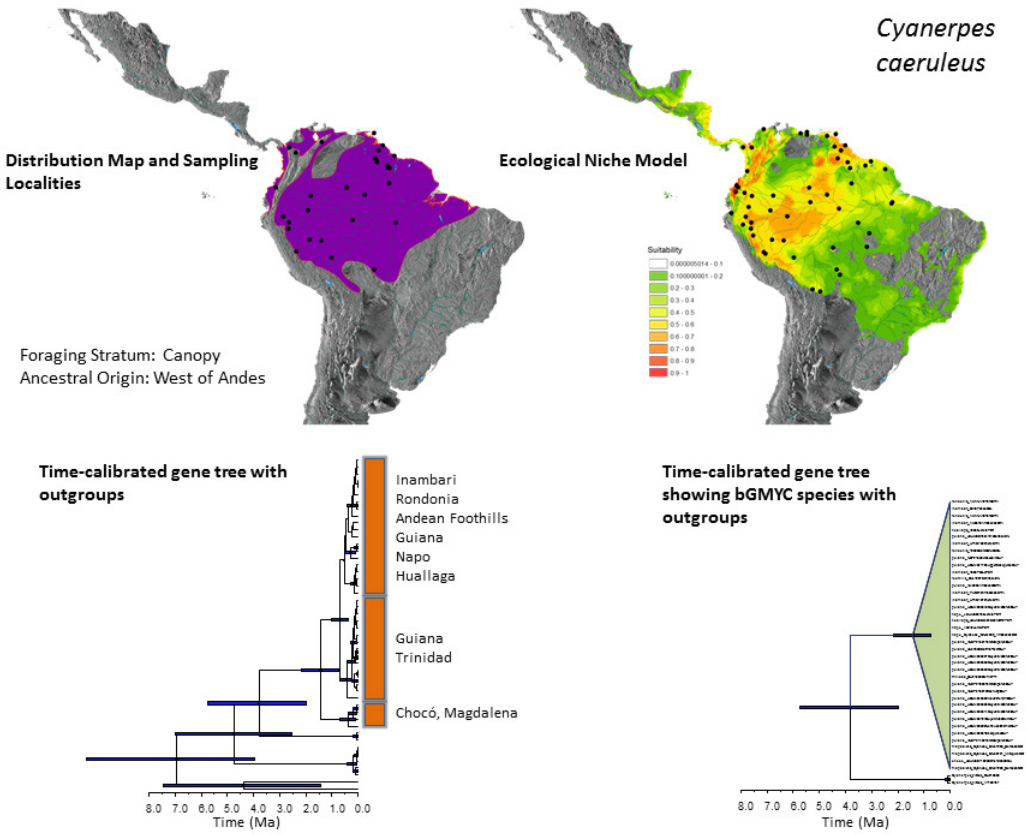

Supplementary Figure 6 | Range map, ENM, time-calibrated gene trees and delimited species for *Cyanerpes caeruleus.* Range map (natureserv.org) showing approximate geographic distribution of each lineage with sampling localities as black circles (upper left). Ecological niche model (ENM) indicating areas with suitable climatic conditions from 0 (clear) to 1.0 (red); locality records used to construct the ENM appear as black circles (upper right). Time-calibrated gene tree showing geographic clades (bottom left). Time-calibrated gene tree with clades collapsed to show species delimited using bGMYC (bottom right).

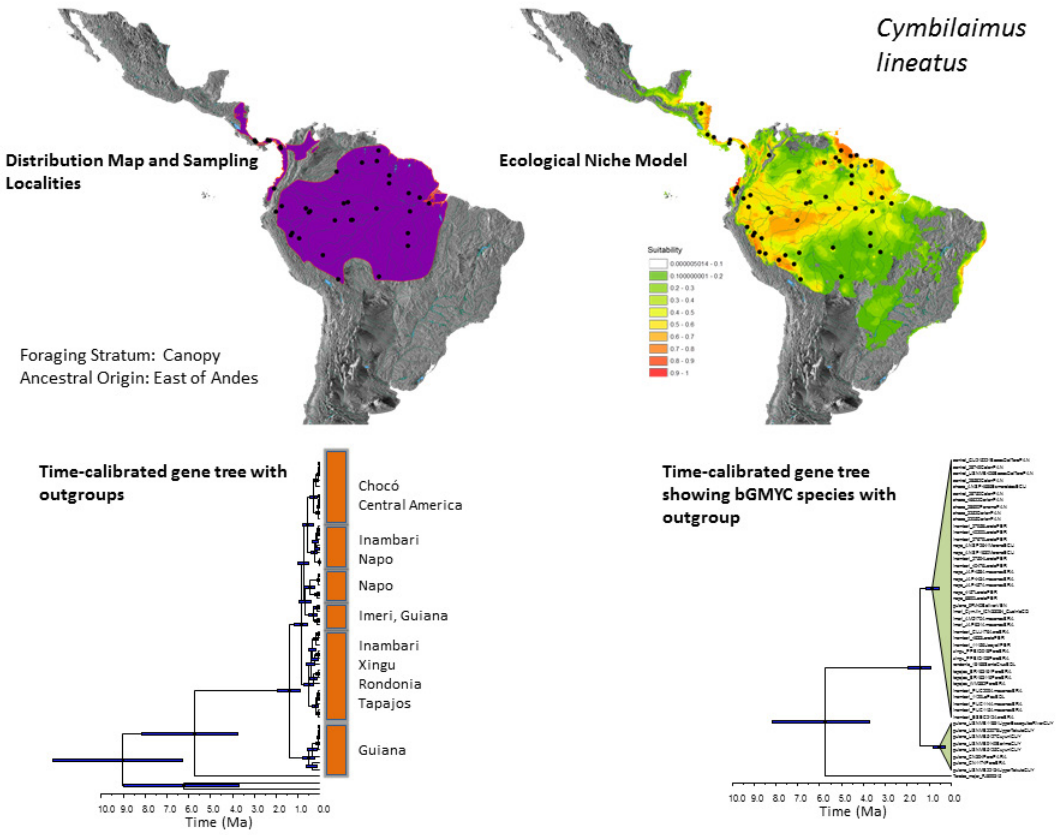

Supplementary Figure 7 | Range map, ENM, time-calibrated gene trees and delimited species for *Cymbilaimus lineatus.* Range map (natureserv.org) showing approximate geographic distribution of each lineage with sampling localities as black circles (upper left). Ecological niche model (ENM) indicating areas with suitable climatic conditions from 0 (clear) to 1.0 (red); locality records used to construct the ENM appear as black circles (upper right). Time-calibrated gene tree showing geographic clades (bottom left). Time-calibrated gene tree with clades collapsed to show species delimited using bGMYC (bottom right).

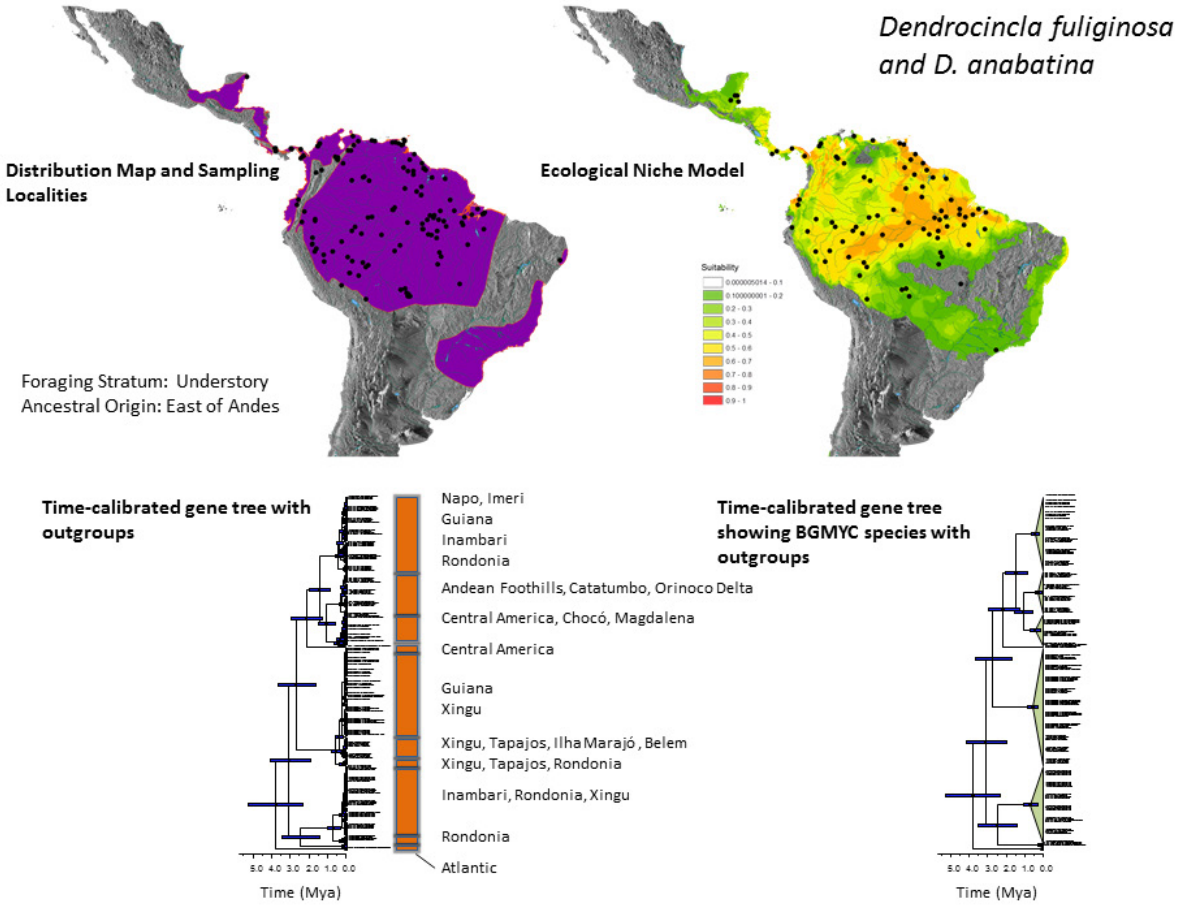

Supplementary Figure 8 | Range map, ENM, time-calibrated gene trees and delimited species for *Dendrocincla fuliginosa*. Ingroup includes *D. fuliginosa* and *D. anabatina*. Range map (natureserv.org) showing approximate geographic distribution of each lineage with sampling localities as black circles (upper left). Ecological niche model (ENM) indicating areas with suitable climatic conditions from 0 (clear) to 1.0 (red); locality records used to construct the ENM appear as black circles (upper right). Time-calibrated gene tree showing geographic clades (bottom left). Time-calibrated gene tree with clades collapsed to show species delimited using bGMYC (bottom right).

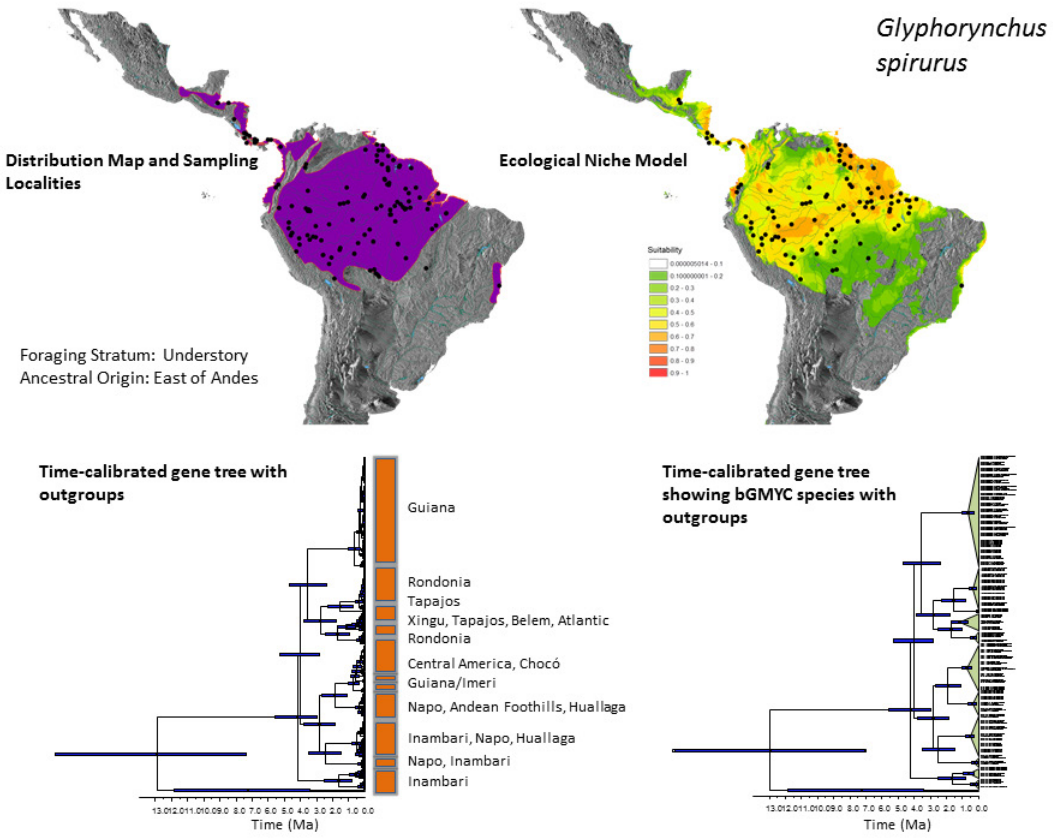

Supplementary Figure 9 | Range map, ENM, time-calibrated gene trees and delimited species for *Glyphorynchus spirurus.* Range map (natureserv.org) showing approximate geographic distribution of each lineage with sampling localities as black circles (upper left). Ecological niche model (ENM) indicating areas with suitable climatic conditions from 0 (clear) to 1.0 (red); locality records used to construct the ENM appear as black circles (upper right). Time-calibrated gene tree showing geographic clades (bottom left). Time-calibrated gene tree with clades collapsed to show species delimited using bGMYC (bottom right).

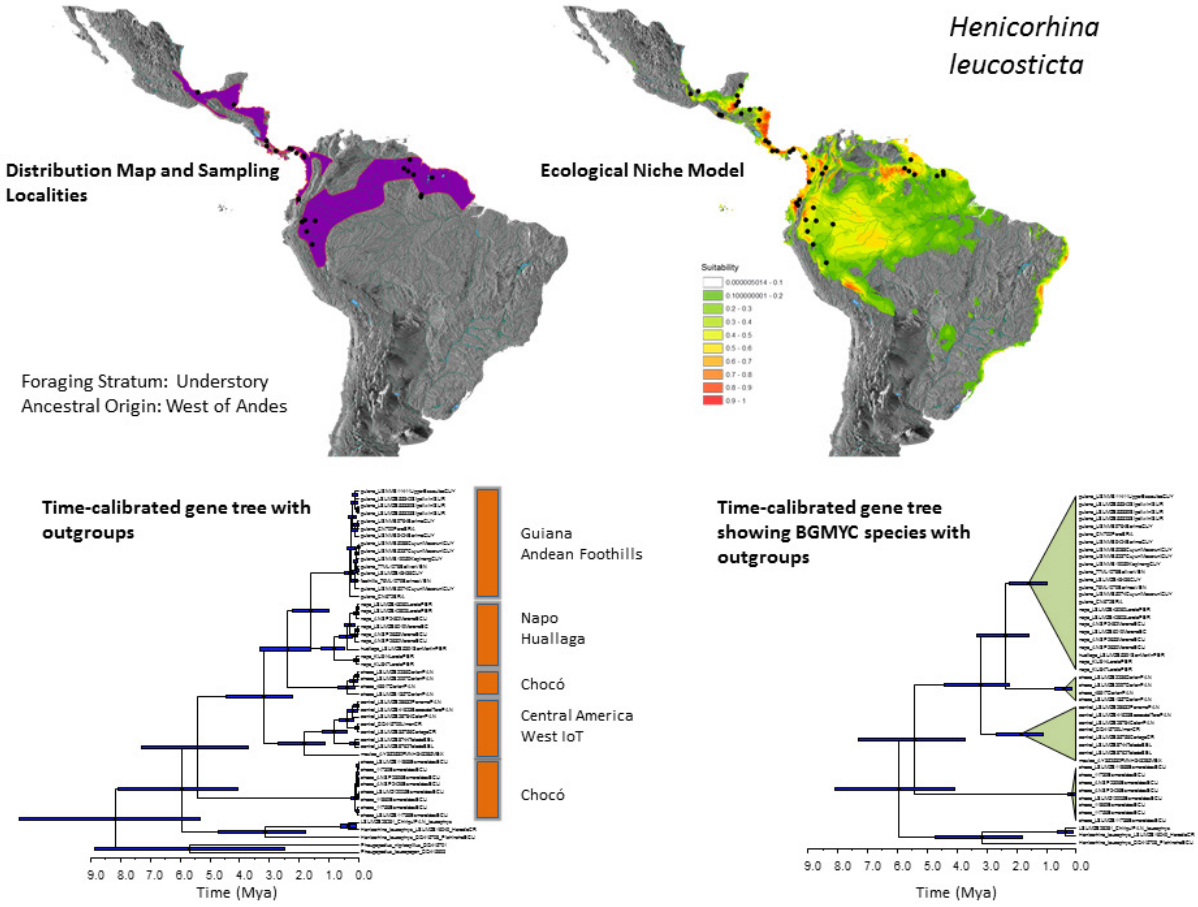

Supplementary Figure 10 | Range map, ENM, time-calibrated gene trees and delimited species for *Henicorhina leucosticta.* Range map (natureserv.org) showing approximate geographic distribution of each lineage with sampling localities as black circles (upper left). Ecological niche model (ENM) indicating areas with suitable climatic conditions from 0 (clear) to 1.0 (red); locality records used to construct the ENM appear as black circles (upper right). Time-calibrated gene tree showing geographic clades (bottom left). Time-calibrated gene tree with clades collapsed to show species delimited using bGMYC (bottom right).

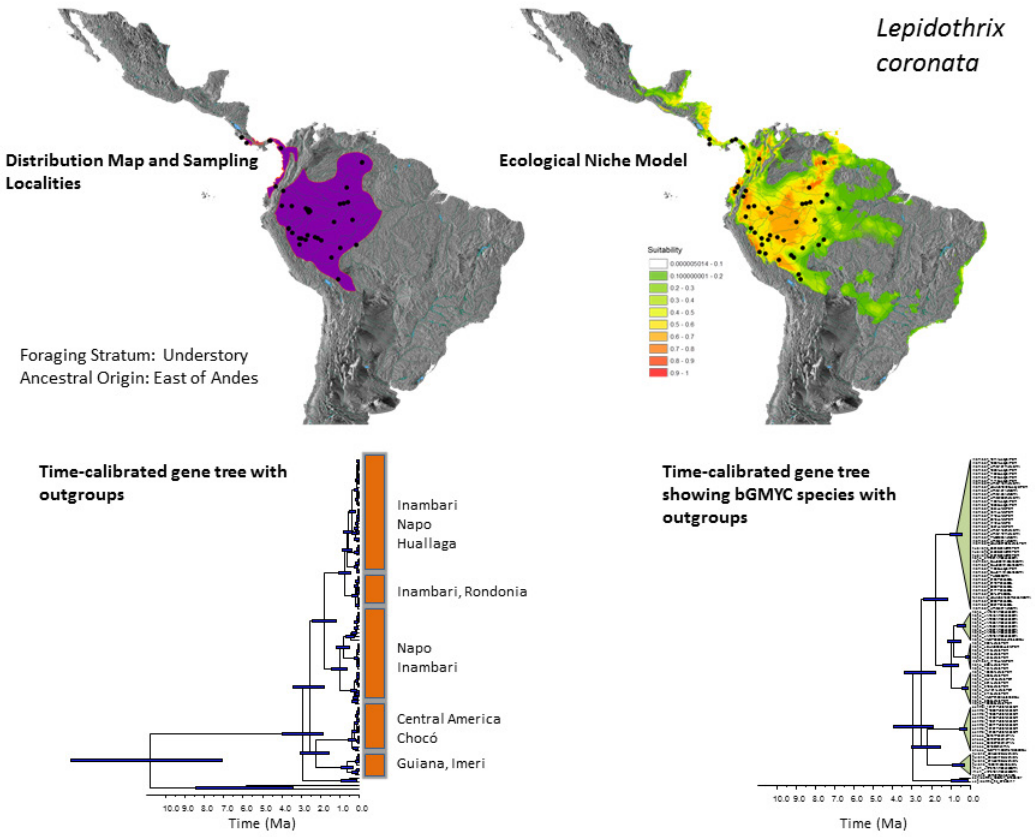

Supplementary Figure 11 | Range map, ENM, time-calibrated gene trees and delimited species for *Lepidothrix coronata.* Range map (natureserv.org) showing approximate geographic distribution of each lineage with sampling localities as black circles (upper left). Ecological niche model (ENM) indicating areas with suitable climatic conditions from 0 (clear) to 1.0 (red); locality records used to construct the ENM appear as black circles (upper right). Time-calibrated gene tree showing geographic clades (bottom left). Time-calibrated gene tree with clades collapsed to show species delimited using bGMYC (bottom right).

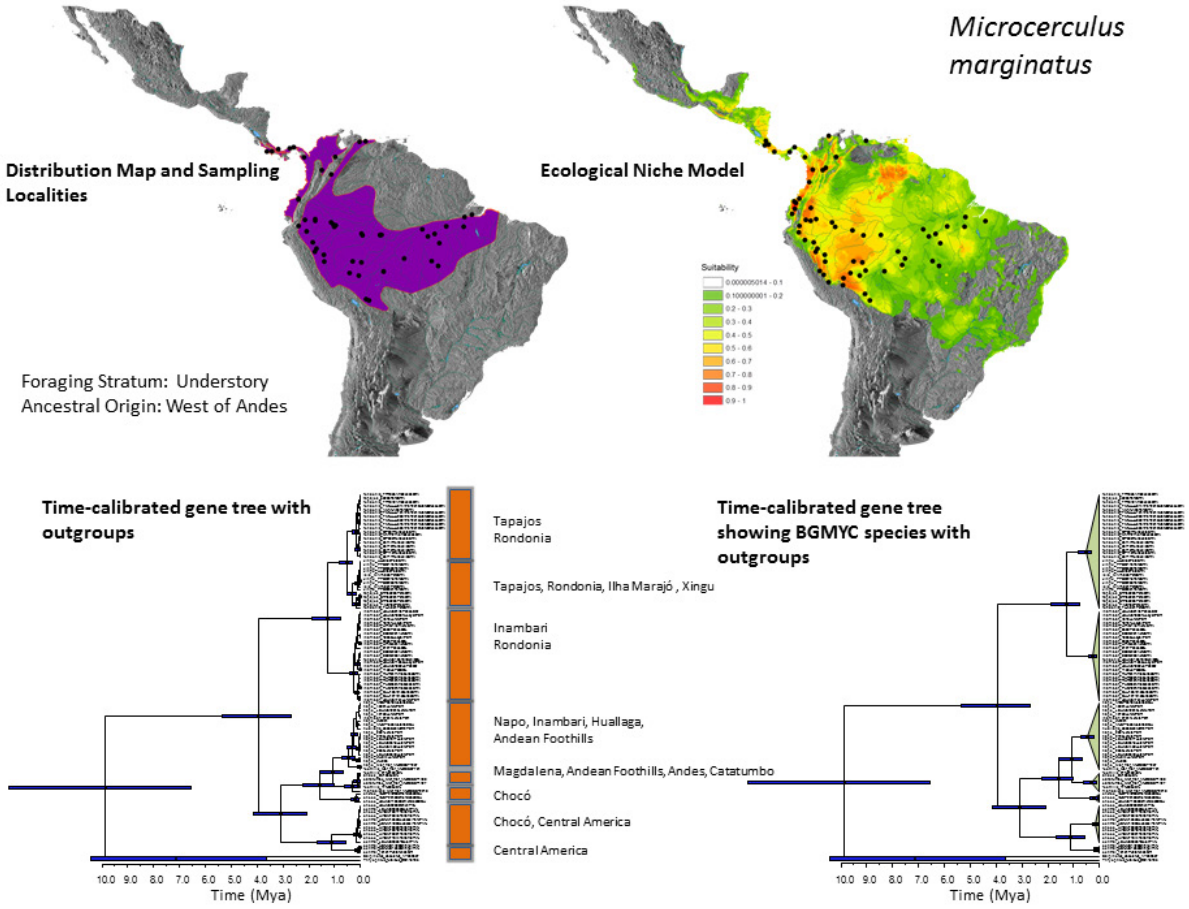

Supplementary Figure 12 | Range map, ENM, time-calibrated gene trees and delimited species for *Microcerculus marginatus.* Range map (natureserv.org) showing approximate geographic distribution of each lineage with sampling localities as black circles (upper left). Ecological niche model (ENM) indicating areas with suitable climatic conditions from 0 (clear) to 1.0 (red); locality records used to construct the ENM appear as black circles (upper right). Time-calibrated gene tree showing geographic clades (bottom left). Time-calibrated gene tree with clades collapsed to show species delimited using bGMYC (bottom right).

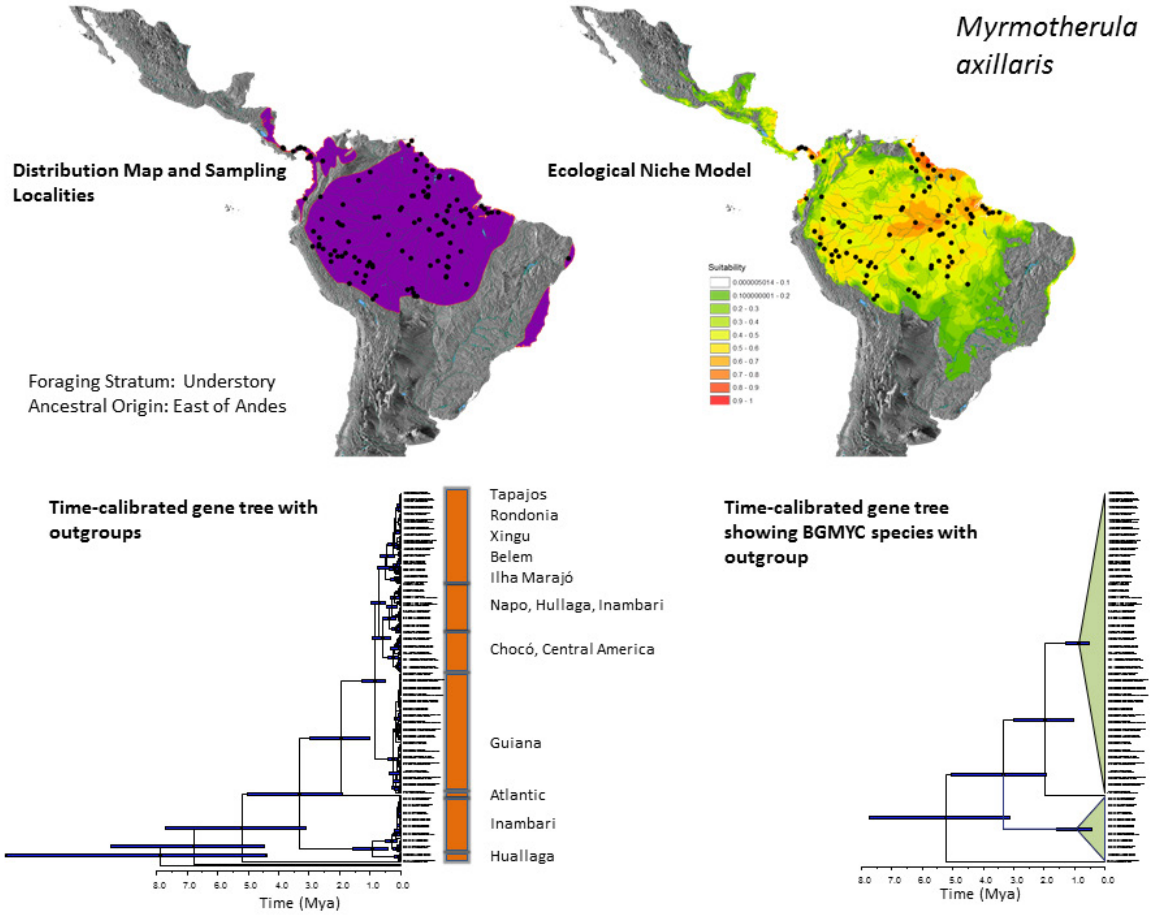

Supplementary Figure 13 | Range map, ENM, time-calibrated gene trees and delimited species for *Myrmotherula axillaris*. Range map (natureserv.org) showing approximate geographic distribution of each lineage with sampling localities as black circles (upper left). Ecological niche model (ENM) indicating areas with suitable climatic conditions from 0 (clear) to 1.0 (red); locality records used to construct the ENM appear as black circles (upper right). Time-calibrated gene tree showing geographic clades (bottom left). Time-calibrated gene tree with clades collapsed to show species delimited using bGMYC (bottom right).

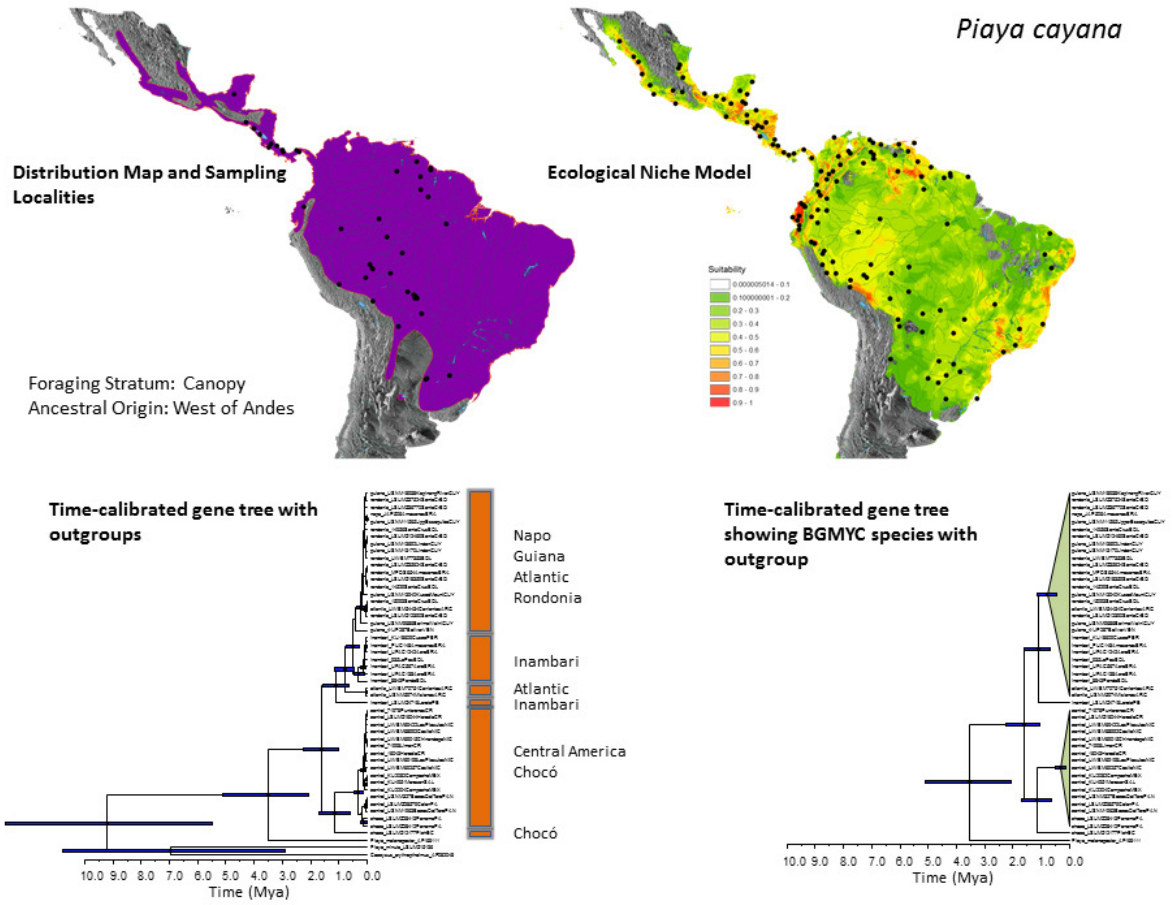

Supplementary Figure 14 | Range map, ENM, time-calibrated gene trees and delimited species for *Piaya cayana*. Range map (natureserv.org) showing approximate geographic distribution of each lineage with sampling localities as black circles (upper left). Ecological niche model (ENM) indicating areas with suitable climatic conditions from 0 (clear) to 1.0 (red); locality records used to construct the ENM appear as black circles (upper right). Time-calibrated gene tree showing geographic clades (bottom left). Time-calibrated gene tree with clades collapsed to show species delimited using bGMYC (bottom right).

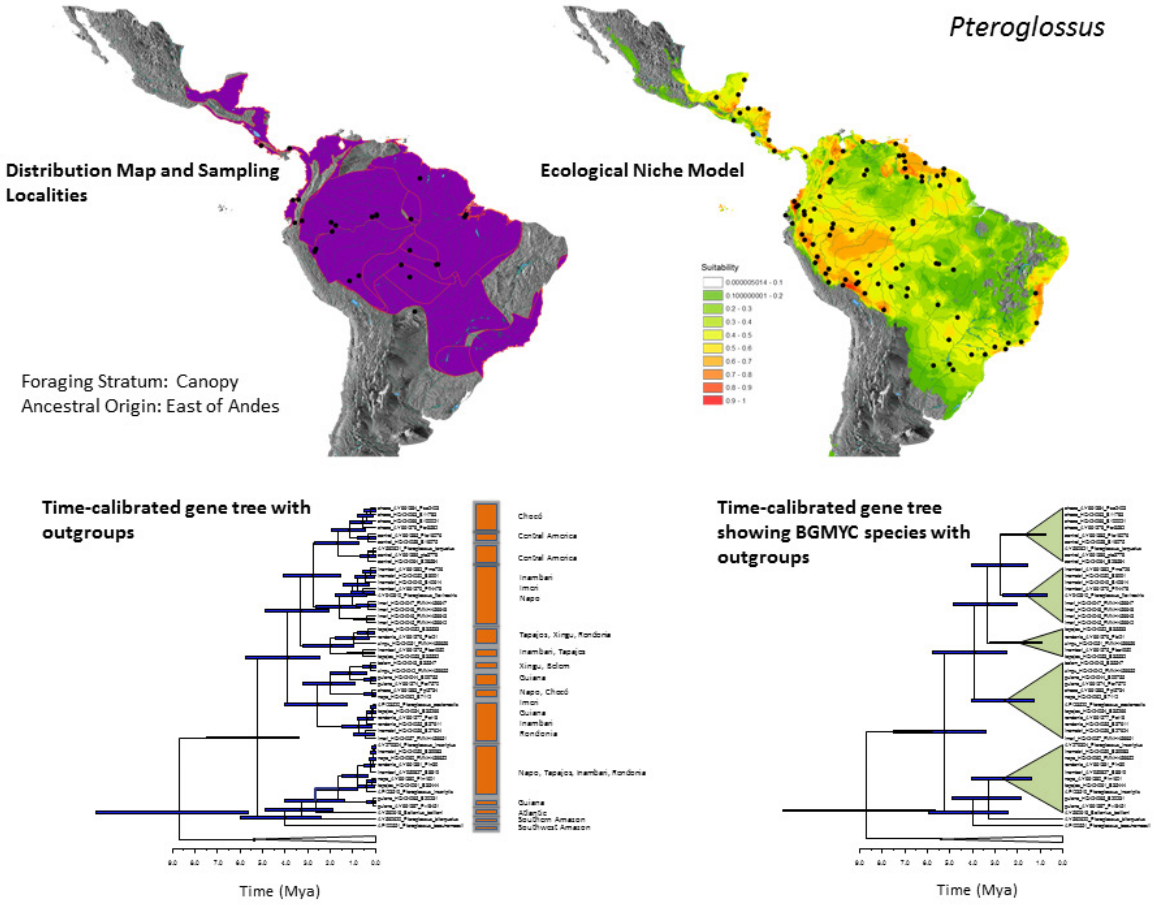

Supplementary Figure 15 | Range map, ENM, time-calibrated gene trees and delimited species for *Pteroglossus.* Ingroup includes all biological species in *Pteroglossus*: *P. azara, viridis, inscriptus, P. bitorquatus, P. aracari, P. castanotis, P. pluricinctus, P. torquatus, P. frantzii, P. beauharnaesii,* and *P. bailloni*. Range map (natureserv.org) showing approximate geographic distribution of each lineage with sampling localities as black circles (upper left). Ecological niche model (ENM) indicating areas with suitable climatic conditions from 0 (clear) to 1.0 (red); locality records used to construct the ENM appear as black circles (upper right). Time-calibrated gene tree showing geographic clades (bottom left). Time-calibrated gene tree with clades collapsed to show species delimited using bGMYC (bottom right).

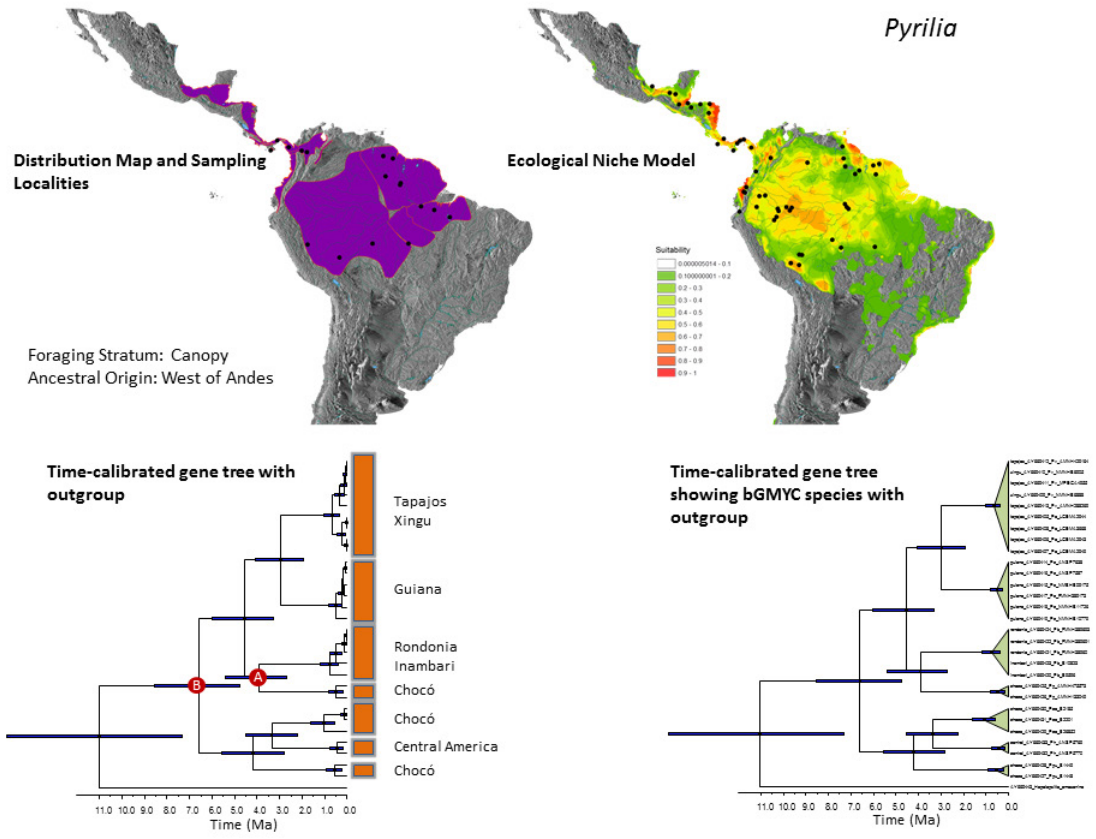

Supplementary Figure 16 | Range map, ENM, time-calibrated gene trees and delimited species for *Pyrilia.* Ingroup includes all biological species in *Pyrilia: P. haematotis, P. pulchra, P. pyrilia, P. barrabandi, P. caica, P. aurantiocephala,* and *P. vulturina.* Range map (natureserv.org) showing approximate geographic distribution of each lineage with sampling localities as black circles (upper left). Ecological niche model (ENM) indicating areas with suitable climatic conditions from 0 (clear) to 1.0 (red); locality records used to construct the ENM appear as black circles (upper right). Time-calibrated gene tree showing geographic clades (bottom left). Time-calibrated gene tree with clades collapsed to show species delimited using bGMYC (bottom right). Nodes labeled A and B refer to multiple cross-Andes divergence events used in the msBayes analysis.

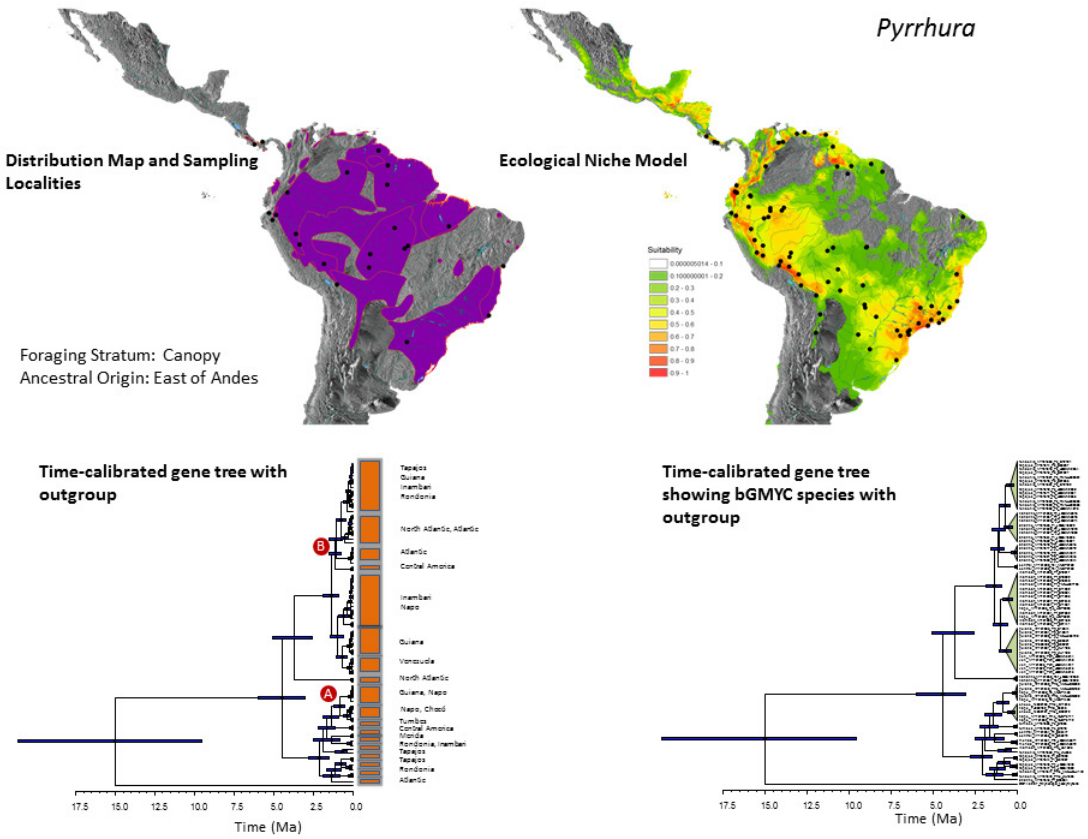

Supplementary Figure 17 | Range map, ENM, time-calibrated gene trees and delimited species for *Pyrrhura*. Ingroup includes all biological species in *Pyrrhura*: *P. roseifrons, P. eisenmanni, P. picta, P. amazonum, P. pfrimeri, P. emma, P. griseipectus, P. leucotis, P. orcesi, P. rhodocephala, P. albipectus, P. molinae, P. frontalis, P. lepida, P. perlata, P. melanura, P. rupicola,* and *P. cruentata*. Range map (natureserv.org) showing approximate geographic distribution of each lineage with sampling localities as black circles (upper left). Ecological niche model (ENM) indicating areas with suitable climatic conditions from 0 (clear) to 1.0 (red); locality records used to construct the ENM appear as black circles (upper right). Time-calibrated gene tree showing geographic clades (bottom left). Time-calibrated gene tree with clades collapsed to show species delimited using bGMYC (bottom right). Nodes labeled A and B refer to multiple cross-Andes divergence events used in the msBayes analysis.

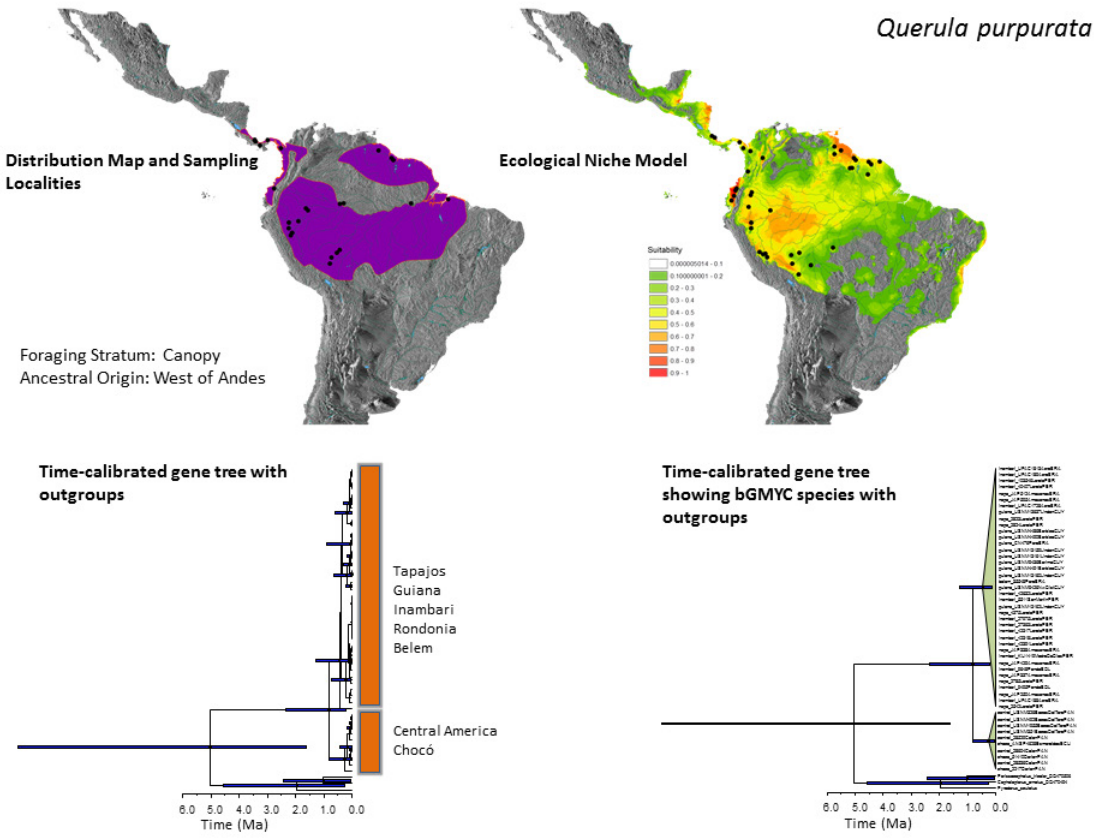

Supplementary Figure 18 | Range map, ENM, time-calibrated gene trees and delimited species for *Querula purpurata.* Range map (natureserv.org) showing approximate geographic distribution of each lineage with sampling localities as black circles (upper left). Ecological niche model (ENM) indicating areas with suitable climatic conditions from 0 (clear) to 1.0 (red); locality records used to construct the ENM appear as black circles (upper right). Time-calibrated gene tree showing geographic clades (bottom left). Time-calibrated gene tree with clades collapsed to show species delimited using bGMYC (bottom right).

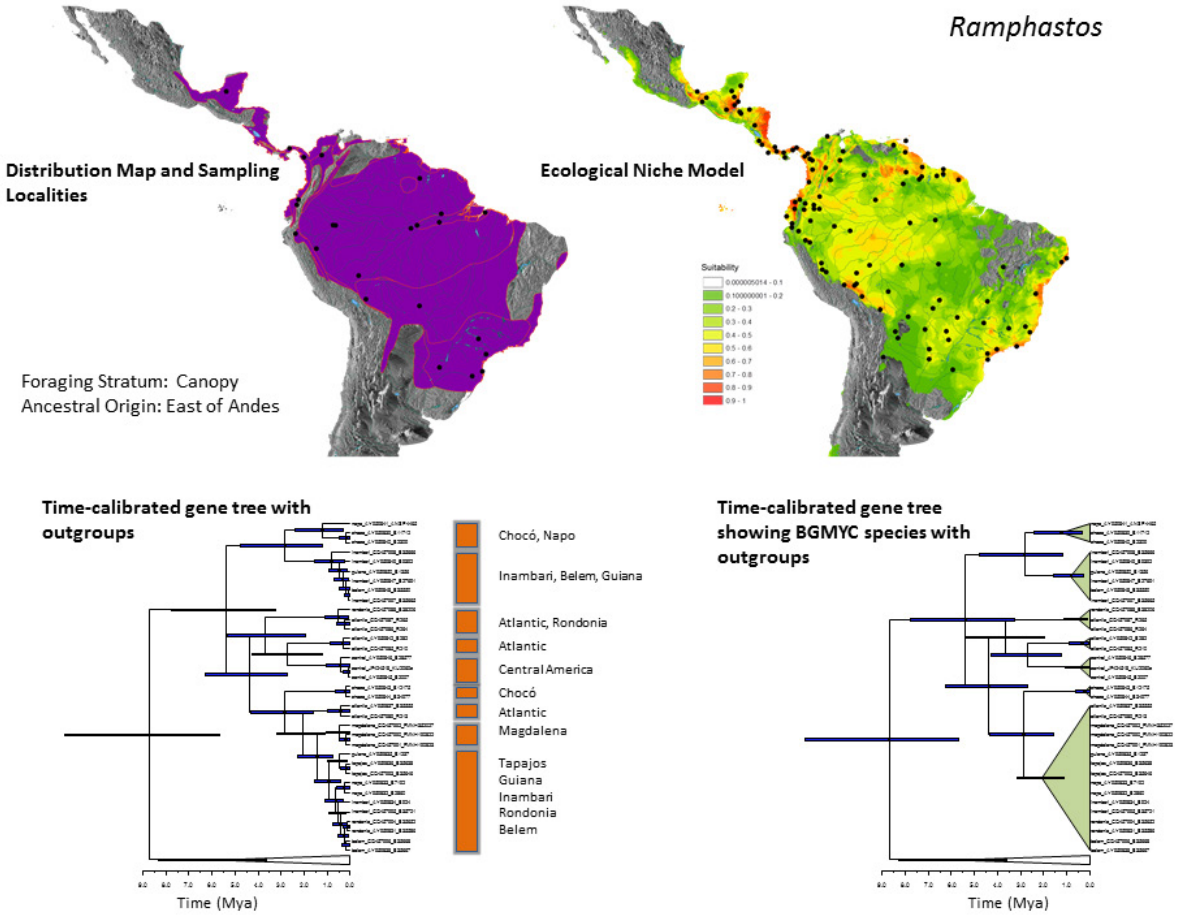

Supplementary Figure 19 | Range map, ENM, time-calibrated gene trees and delimited species for *Ramphastos.* Ingroup includes all biological species in *Ramphastos: R. sulfuratus, R. brevis, R. vitellinus, R. dicolorus, R. ambiguus , R. tucanus,* and *R. toco*. Range map (natureserv.org) showing approximate geographic distribution of each lineage with sampling localities as black circles (upper left). Ecological niche model (ENM) indicating areas with suitable climatic conditions from 0 (clear) to 1.0 (red); locality records used to construct the ENM appear as black circles (upper right). Time-calibrated gene tree showing geographic clades (bottom left). Time-calibrated gene tree with clades collapsed to show species delimited using bGMYC (bottom right).

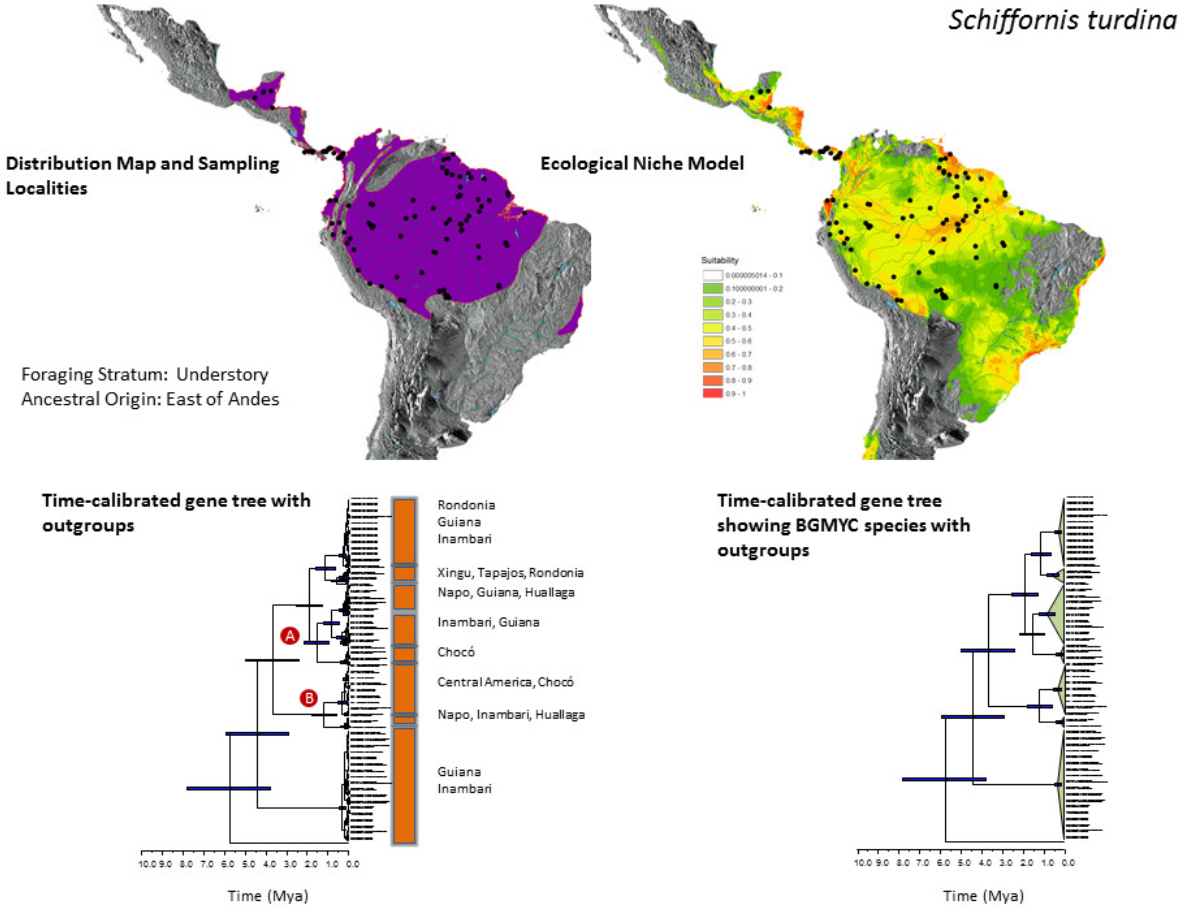

Supplementary Figure 20 | Range map, ENM, time-calibrated gene trees and delimited species for *Schiffornis turdina.* Range map (natureserv.org) showing approximate geographic distribution of each lineage with sampling localities as black circles (upper left). Ecological niche model (ENM) indicating areas with suitable climatic conditions from 0 (clear) to 1.0 (red); locality records used to construct the ENM appear as black circles (upper right). Time-calibrated gene tree showing geographic clades (bottom left). Time-calibrated gene tree with clades collapsed to show species delimited using bGMYC (bottom right). Nodes labeled A and B refer to multiple cross-Andes divergence events used in the msBayes analysis.

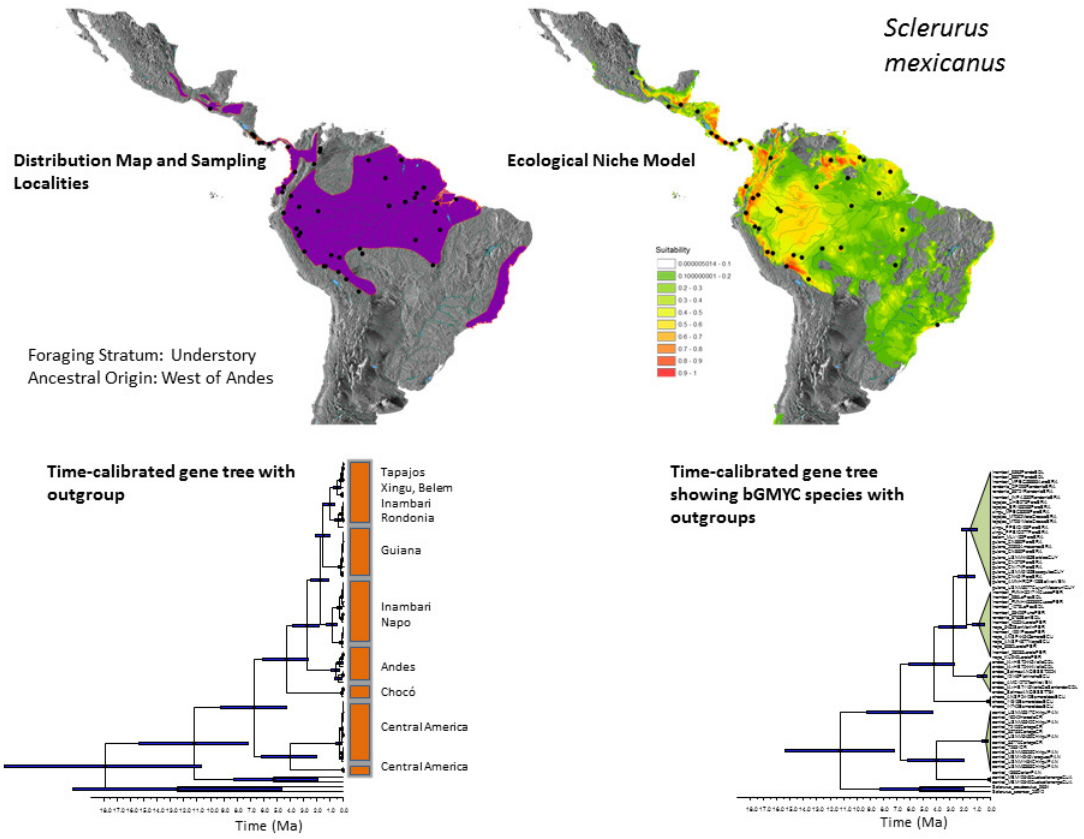

Supplementary Figure 21| Range map, ENM, time-calibrated gene trees and delimited species for *Sclerurus mexicanus.* Range map (natureserv.org) showing approximate geographic distribution of each lineage with sampling localities as black circles (upper left). Ecological niche model (ENM) indicating areas with suitable climatic conditions; locality records used to construct the ENM appear as black circles (upper right). Time-calibrated gene tree showing geographic clades (bottom left). Time-calibrated gene tree with clades collapsed to show species delimited using bGMYC (bottom right).

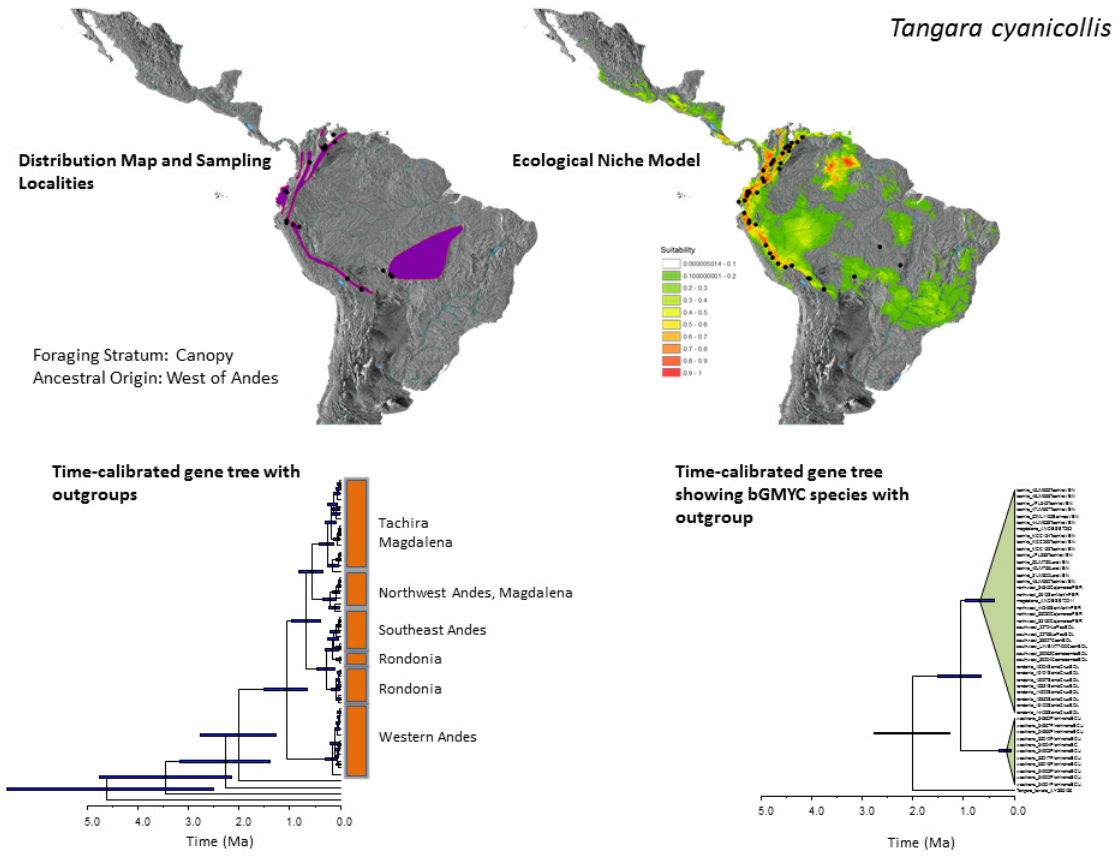

Supplementary Figure 22 | Range map, ENM, time-calibrated gene trees and delimited species for *Tangara cyanicollis*. Range map (natureserv.org) showing approximate geographic distribution of each lineage with sampling localities as black circles (upper left). Ecological niche model (ENM) indicating areas with suitable climatic conditions from 0 (clear) to 1.0 (red); locality records used to construct the ENM appear as black circles (upper right). Time-calibrated gene tree showing geographic clades (bottom left). Time-calibrated gene tree with clades collapsed to show species delimited using bGMYC (bottom right).

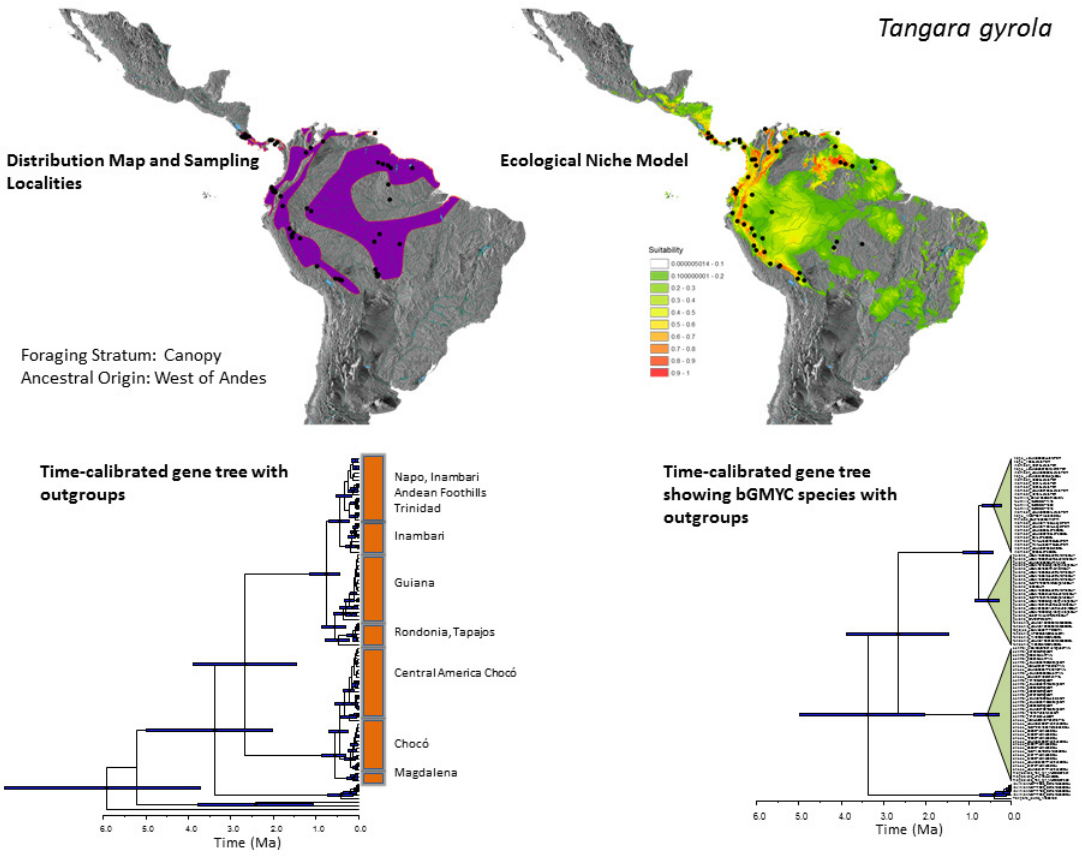

Supplementary Figure 23 | Range map, ENM, time-calibrated gene trees and delimited species for *Tangara gyrola.* Range map (natureserv.org) showing approximate geographic distribution of each lineage with sampling localities as black circles (upper left). Ecological niche model (ENM) indicating areas with suitable climatic conditions from 0 (clear) to 1.0 (red); locality records used to construct the ENM appear as black circles (upper right). Time-calibrated gene tree showing geographic clades (bottom left). Time-calibrated gene tree with clades collapsed to show species delimited using bGMYC (bottom right).

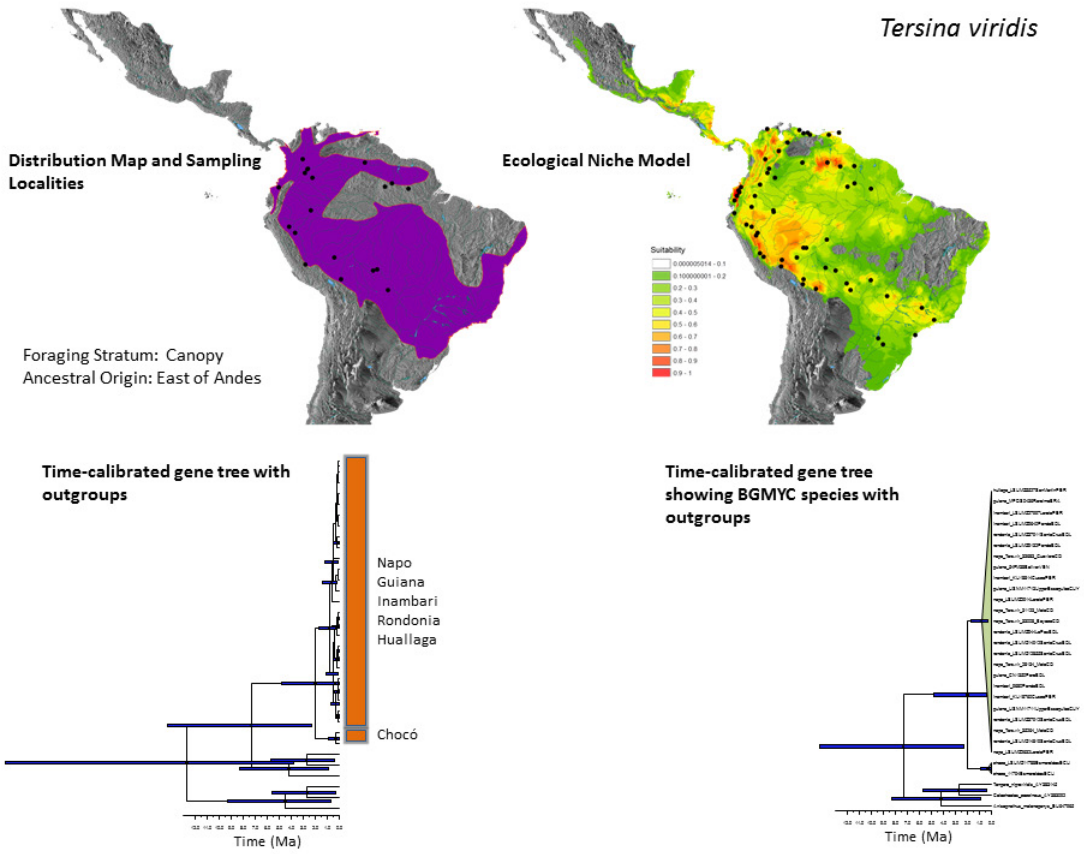

Supplementary Figure 24 | Range map, ENM, time-calibrated gene trees and delimited species for *Tersina viridis.* Range map (natureserv.org) showing approximate geographic distribution of each lineage with sampling localities as black circles (upper left). Ecological niche model (ENM) indicating areas with suitable climatic conditions from 0 (clear) to 1.0 (red); locality records used to construct the ENM appear as black circles (upper right). Time-calibrated gene tree showing geographic clades (bottom left). Time-calibrated gene tree with clades collapsed to show species delimited using bGMYC (bottom right).

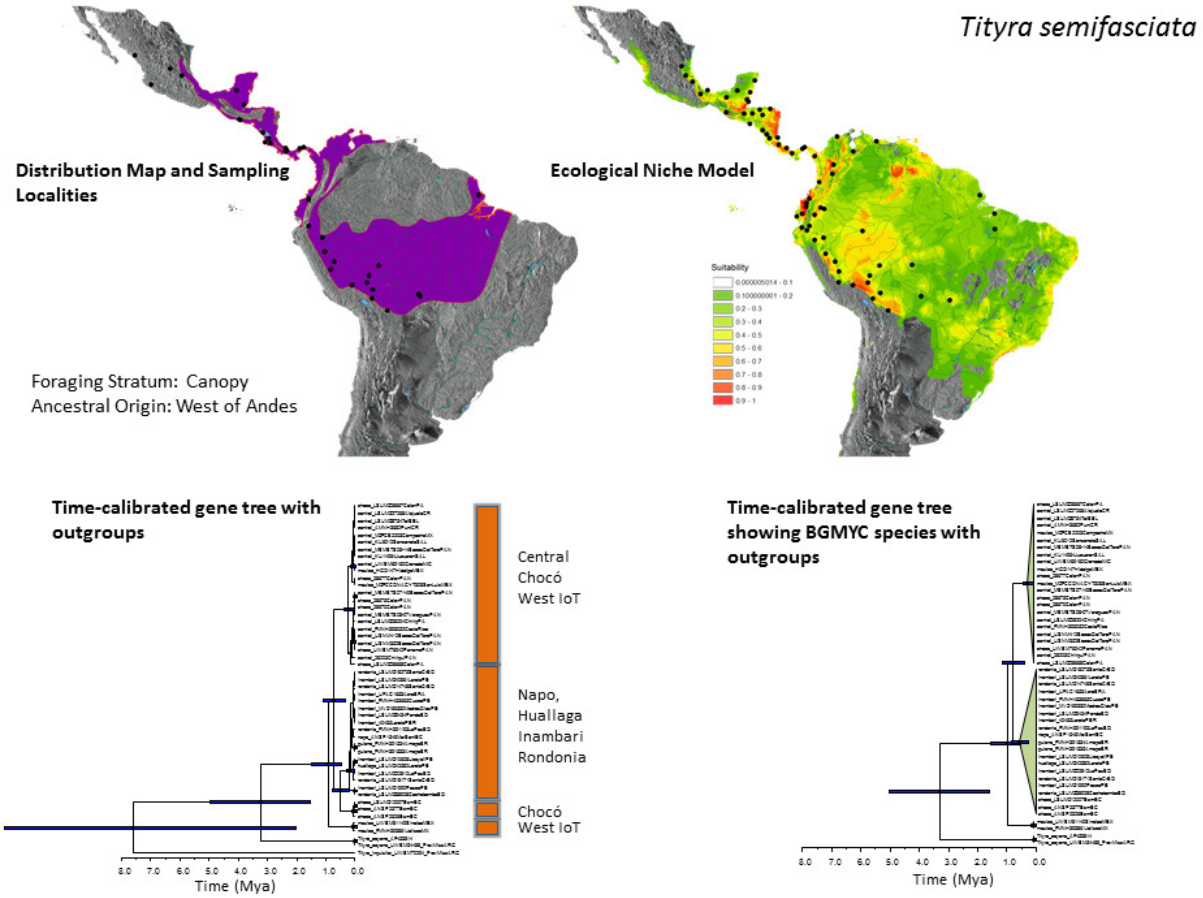

Supplementary Figure 25 | Range map, ENM, time-calibrated gene trees and delimited species for *Tityra semifaciata.* Range map (natureserv.org) showing approximate geographic distribution of each lineage with sampling localities as black circles (upper left). Ecological niche model (ENM) indicating areas with suitable climatic conditions from 0 (clear) to 1.0 (red); locality records used to construct the ENM appear as black circles (upper right). Time-calibrated gene tree showing geographic clades (bottom left). Time-calibrated gene tree with clades collapsed to show species delimited using bGMYC (bottom right).

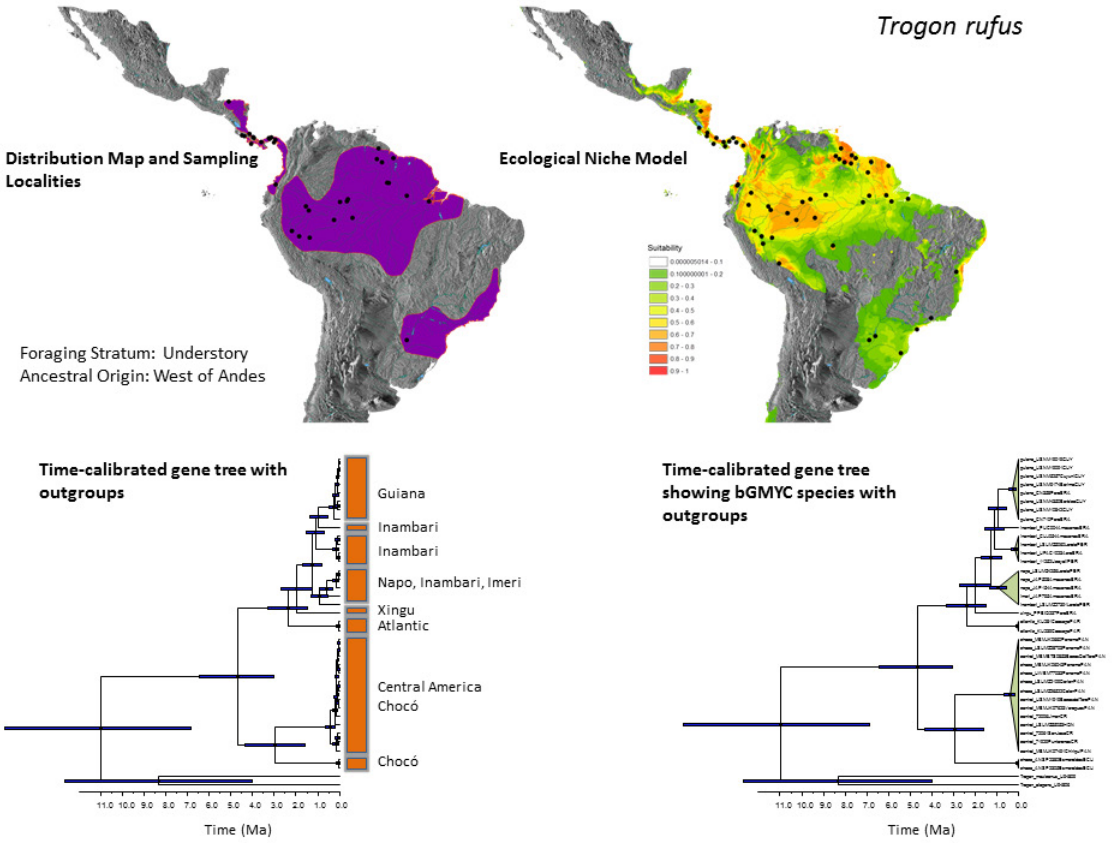

Supplementary Figure 26 | Range map, ENM, time-calibrated gene trees and delimited species for *Trogon rufus*. Range map (natureserv.org) showing approximate geographic distribution of each lineage with sampling localities as black circles (upper left). Ecological niche model (ENM) indicating areas with suitable climatic conditions from 0 (clear) to 1.0 (red); locality records used to construct the ENM appear as black circles (upper right). Time-calibrated gene tree showing geographic clades (bottom left). Time-calibrated gene tree with clades collapsed to show species delimited using bGMYC (bottom right).

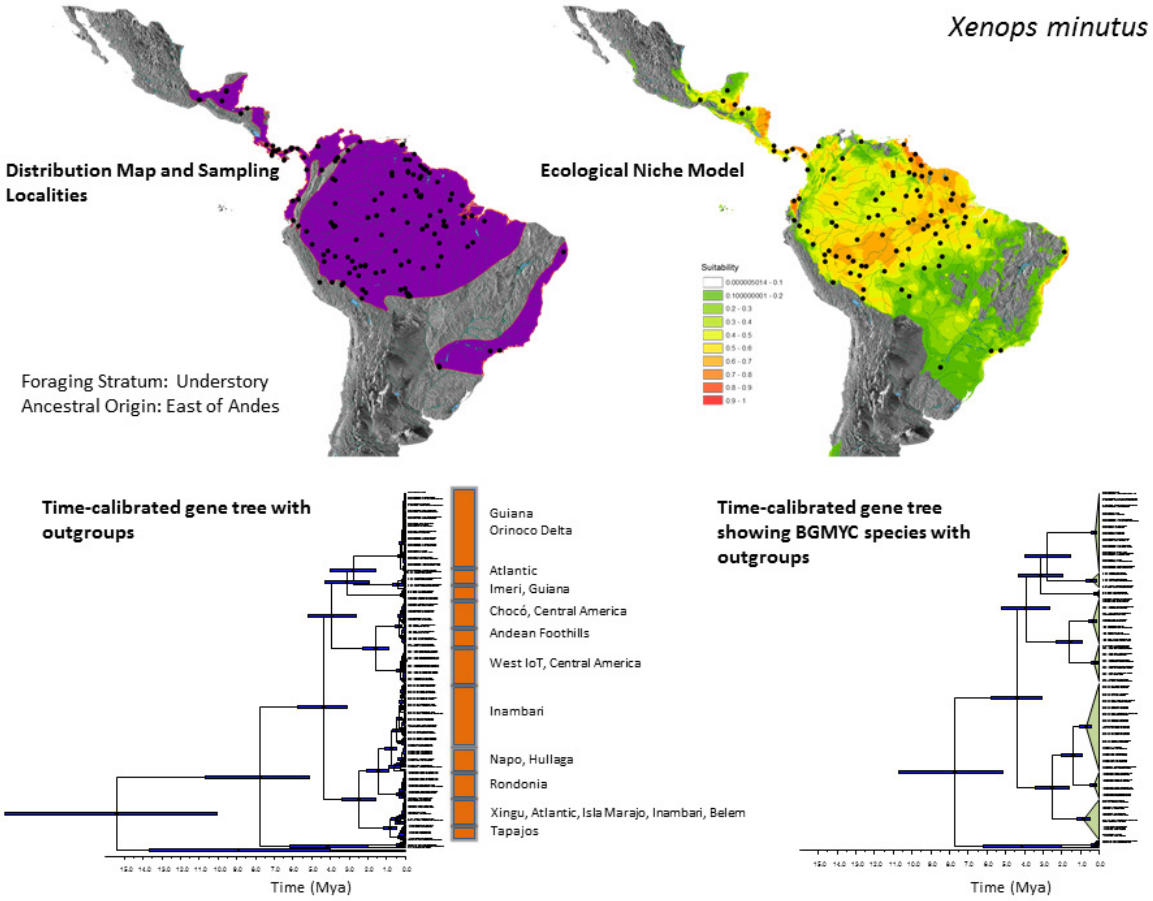

Supplementary Figure 27 | Range map, ENM, time-calibrated gene trees and delimited species for *Xenops minutus.* Range map (natureserv.org) showing approximate geographic distribution of each lineage with sampling localities as black circles (upper left). Ecological niche model (ENM) indicating areas with suitable climatic conditions from 0 (clear) to 1.0 (red); locality records used to construct the ENM appear as black circles (upper right). Time-calibrated gene tree showing geographic clades (bottom left). Time-calibrated gene tree with clades collapsed to show species delimited using bGMYC (bottom right).

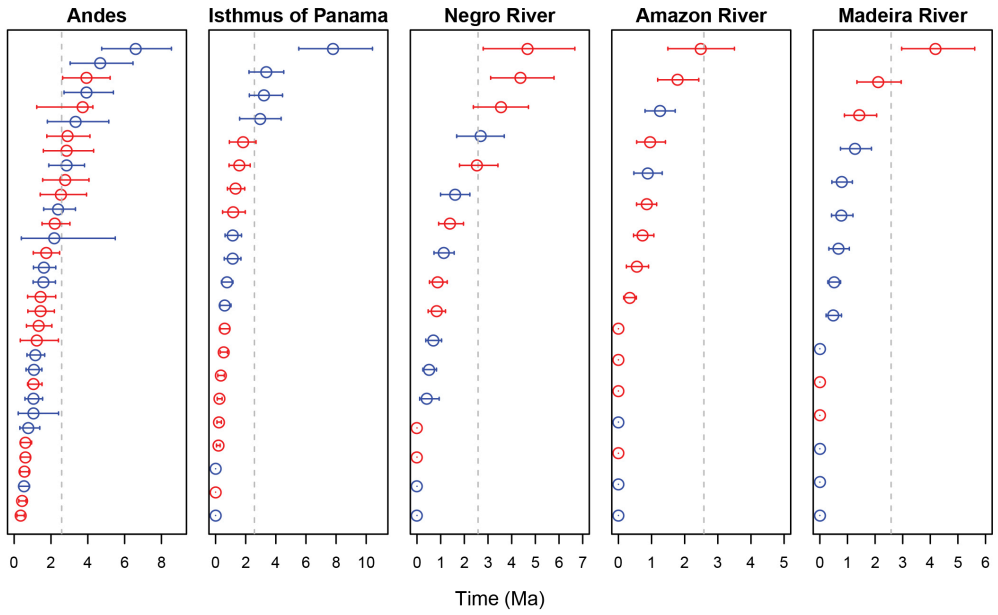

Supplementary Figure 28 | Plot showing patterns of divergence times and ancestral geographical origin across each of the major landscape barriers. Divergence times were inferred from BEAST analyses. Points are colour coded by a lineage's ancestral geographical origin: west of the Andes (blue) or east of the Andes (red). Circles represent mean estimates and bars represent the 95% highest posterior density. Vertical hashed lines at 2.58 million years represent the transition between the Neogene and Quaternary periods.